The genomic landscape, causes, and consequences of extensive phylogenomic discordance in ~~Old World mice and rats~~murine rodents

Gregg W. C. Thomas[1,2,*], Jonathan J. Hughes[3,4], Tomohiro Kumon[5], Jacob S. Berv[3,6], C. Erik Nordgren[5], Michael Lampson[5], Mia Levine[5], Jeremy B. Searle[3], Jeffrey M. Good[1]

[1]*Division of Biological Sciences, University of Montana, Missoula, MT, 59801.*

[2]*Informatics Group, Harvard University, Cambridge, MA, 02138*

[3]*Department of Ecology and Evolutionary Biology, Cornell University, Ithaca, NY, 14853.*

[4]*Department of Evolution, Ecology, and Organismal Biology, University of California Riverside, Riverside, CA, 92521*

[5]*Department of Biology, University of Pennsylvania, Philadelphia, PA, 19104*

[6] *Department of Ecology and Evolutionary Biology, University of Michigan, Ann Arbor, MI, 48109*

[*]Corresponding author

E-mail: gthomas@fas.harvard.edu

Abstract

A species tree is a central concept in evolutionary biology whereby a single branching phylogeny reflects relationships among species. However, the phylogenies of different genomic regions often differ from the species tree. Although tree discordance is widespread in phylogenomic studies, we still lack a clear understanding of how variation in phylogenetic patterns is shaped by genome biology or the extent to which discordance may compromise comparative studies. We characterized patterns of phylogenomic discordance across the murine rodents ~~(Old World mice and rats) –~~ a large and ecologically diverse group that gave rise to the laboratory mouse and rat model systems. Combining recently published linked-read genome assemblies for seven murine species with other available rodent genomes, we first used ultra-conserved elements (UCEs) to infer a robust time-calibrated species tree. We then used whole genomes to examine finer-scale patterns of discordance ~~and~~across 12 million years of divergence. We found that proximate chromosomal regions tended to have more similar phylogenetic histories~~. While we found~~, but no clear relationship between local tree similarity and recombination rates in house mice. However, we did observe a correlation between recombination rates and average similarity to the species tree. We also detected a strong influence of linked selection whereby purifying selection at UCEs led to appreciably less discordance. Finally, we show that assuming a single species tree can result in high error rates when testing for positive selection under different models. Collectively, our results highlight the complex relationship between phylogenetic inference and genome biology and underscore how failure to account for this complexity can mislead comparative genomic studies.

Keywords: *phylogenetic discordance, murine rodents, molecular evolution recombination, genomics, mouse*

Significance Statement

Genomic data has demonstrated that when sequences from multiple species are compared, different regions of the genome exhibit different phylogenetic histories. These discordant histories could be due to either biological processes, such as ancestral variation or introgression, or artifacts of the inference process. We use the genomes of several murine rodents to distinguish how features of the genome, such as recombination rates, genes, and other conserved regions, affect this discordance across the genome. Considering the prevalence of discordance across the genome, we also test how using a single species tree, a common practice, affects inferences from tests for positive selection. Our study shows that conserved genomic loci exhibit lower amounts of discordance, and that discordance can negatively affect inferences of selection when the incorrect species tree is used.

Introduction

Phylogenies are the unifying concept in understanding the evolution of species, traits, and genes. However, ~~with the availability of~~ extensive high-throughput sequencing data ~~it~~ has ~~become apparent~~now revealed that evolutionary relationships between species may not be well represented by a single representative phylogeny (Edwards 2009; Hahn and Nakhleh 2016). While a dominant signal of bifurcating speciation ~~may exist~~usually exists (*i.e.*, a species tree), phylogenetic signal that may disagree with species relationships can arise from ancestral polymorphisms (incomplete lineage sorting; ILS), gene flow ~~through hybridization~~ (introgression), and gene duplication and loss (Maddison 1997). The theoretical prediction of phylogenetic discordance has long been appreciated (Hudson 1983; Pamilo and Nei 1988; Maddison 1997; Rosenberg 2002), but empirical evidence now emphasizes just how extensive discordance can be among a set of species~~. Several recent studies focused on analyzing phylogenetic discordance among the genomes of specific taxonomic groups~~ (Feng, et al. 2022; Gable, et al. 2022; Smith, et al. 2023). ~~Among others~~For example, studies of birds (Jarvis, et al. 2014), ~~seals~~mammals (Ferreira, et al. 2021; Lopes, et al. 2021; Foley, et al. 2024), ~~tomatoes~~plants (Pease, et al. 2016)~~, bumblebees~~ (Pease, et al. 2016), and insects (Sun, et al. 2021; He, et al. 2023)~~, and butterflies~~ (He, et al. 2023) have found that with extensive taxon sampling and genomic data, highly supported species tree topologies are rarely or never recovered in the underlying locus trees. Whereas these examples highlight the prevalence of phylogenetic discordance across the tree of life, we still lack a clear understanding of how phylogenetic patterns are shaped by the details of genome biology or the extent to which discordance may compromise inferences from comparative studies that assume a singular species history.

~~From a practical perspective~~ In practice, failure to acknowledge and account for phylogenetic discordance could severely affect biological inference. Analyses of molecular evolution are usually performed on a gene-by-gene basis (Pond, et al. 2005; Yang 2007; Hu, et al. 2019; Kowalczyk, et al. 2019), but it is still common practice to assume a single genome-wide species tree for each locus. For gene-based analyses, using the wrong tree may ~~compromise~~cause erroneous inferences of positive directional selection, convergent evolution, and genome-wide inferences of correlated rate variation (Mendes, et al. 2016). Phylogenetic discordance can also affect how continuous traits are reconstructed across phylogenies, as the genes that underly these traits may not follow the species history (Avise and Robinson 2008; Hahn and Nakhleh 2016; Mendes, et al. 2018; Hibbins, et al. 2023). In these instances, phylogenetic discordance may need to be characterized and incorporated into the experimental and analytical design. Alternatively, if a researcher's primary questions are focused on reconstructing the evolutionary history of speciation (*i.e.*, the species tree), then phylogenetic discordance may obscure the true signal of speciation (Fontaine, et al. 2015; Foley, et al. 2024). In this case, knowledge about patterns of discordance across genomes could inform decisions about locus selection, data filtering, and model parameters during species tree reconstruction.

Given these considerations, a better understanding of the genomic context of phylogenetic discordance is warranted. Although often conceptualized primarily as a stochastic consequence of

population history (Maddison 1997), patterns of phylogenetic discordance are likely to be non-random and dependent on localized patterns of genetic drift, natural selection, recombination, and mutation. Discordance due to ILS ultimately depends on effective population sizes across the branches of the phylogeny (Pamilo and Nei 1988; Degnan and Rosenberg 2006) and, therefore, should covary with any process that influences local patterns of genetic diversity (*e.g.*, linked negative or positive selection). Likewise, ~~the potential for~~ discordance due to introgression may be influenced by selection against incompatible alleles or positive selection for beneficial variants (Lewontin and Birch 1966; Jones, et al. 2018). Selection, ILS, and introgression, are expected to leave ~~differing~~different genomic signals ~~across a sample of genomes~~ that should allow us to test hypotheses about both the cause and the scale of phylogenetic discordance (Huson, et al. 2005; Kulathinal, et al. 2009; Green, et al. 2010; Vanderpool, et al. 2020). Yet the genomic context of phylogenetic discordance has remained elusive. For example, localized patterns of phylogenetic discordance should be influenced by patterns of recombination (Hudson and Kaplan 1988) and simulation studies ~~posit~~confirm that the closer two regions are in the genome, the more history they share (Slatkin and Pollack 2006; McKenzie and Eaton 2020). However, empirical studies ~~of mammals~~ have been inconclusive regarding the relationship between ~~phylogenetic~~ discordance and recombination rates, ranging from no ~~correlation~~relationship in great apes (Hobolth, et al. 2007) ~~to~~, a weak positive correlation in house mice (White, et al. 2009). ~~Some studies have also linked increased amounts of phylogenetic discordance to areas of the genome with lower recombination rates~~ (White, et al. 2009), a strong positive correlation broadly across primates (Rivas-Gonzalez, et al. (2023). ~~More recently,~~ , or increased discordance in regions of lower recombination (Scally, et al. 2012; Pease and Hahn 2013) ~~have found a strong correlation between levels of ILS and recombination rate through a detailed study of the primate phylogeny. However~~. Thus, it remains unclear how phylogenetic discordance scales locally across the genome as a function of recombination and the strength of linked selection~~.~~, pointing to the need for empirical studies in systems with sufficient genomic resources to explore the causes of discordance.

To investigate the causes and consequences of phylogenetic discordance, we took advantage of genomic resources available for house ~~mouse~~mice (*Mus musculus*). This rodent species is one of the most important mammalian model systems for biological and biomedical research and is embedded within a massive radiation of ~~Old World~~ rats and mice (Murinae). This ecologically diverse and species-rich group is comprised of over 600 species and makes up >10% of all mammalian species, and yet is only about 15 million years old~~.~~, making this system an excellent choice for phylogenetic studies over both short and long timescales. Despite the power of evolution-guided functional and biomedical analysis (Christmas, et al. 2023), relatively few murine genomes have been sequenced outside of *Mus* and *Rattus*.

~~In the present work, we~~We analyze recently sequenced ~~genome sequences~~genomes for seven murine ~~rodent~~ species (*Mastomys natalensis*, *Hylomyscus alleni*, *Praomys delectorum*, *Rhabdomys dilectus*, *Grammoyms dolichurus*, *Otomoys typus*, and *Rhynchomys soricoides*) sampled from across this radiation (Kumon, et al. 2021). We combine these new genomes with previously sequenced ~~rodent~~ genomes and genomic resources from the *M. musculus* model system

to study phylogenetic relationships within Murinae as well as the landscape of discordance along rodent chromosomes. We first inferred a species tree for these and other sequenced rodent genomes, focusing on signals derived from commonly used ultra-conserved elements (UCEs~~)~~). We used these UCE data to ~~promote broader comparisons across genomes~~ infer a robust, time-calibrated phylogeny of ~~variable quality. We~~ sequenced murine rodents, providing a useful resource for future comparative studies within this important group. Using this species tree, we then used ~~whole genome sequences from~~ a subset of ~~these genomes,~~whole genomes to study how phylogenetic discordance is related to species-level inferences of relatedness, recombination rate, and patterns of molecular evolution. Using genetic maps~~,~~ and functional annotation ~~information~~ from the powerful house ~~mice to describe the genomic context of phylogenetic discordance across murine rodents and evaluate~~mouse system, we test several hypotheses linking spatial patterns of discordance to genetic drift, natural selection, and recombination. Finally, we show how the use of a single species-tree impacts gene-level inferences from common molecular evolution tests for natural selection in these species. Collectively, our results advance our understanding of how core features of genome biology influence underlying phylogenetic patterns, the extent to which established model system resources can be leveraged for broader phylogenetic studies, and the consequences of ignoring phylogenetic uncertainty.

Results

Estimation of a murine species tree

Using a concatenated dataset of 2,632 aligned ultra conserved elements (UCEs), we inferred a species tree of 18 murine rodent species (Figure~~.~~ 1; Table S1) that recovered the same relationships as previous reconstructions of Murinae using a small number of loci (Lecompte, et al. 2008; Steppan and Schenk 2017). The species tree inferred from a quartet-based summary of the gene tree topologies was identical to the concatenated tree (~~Fig.~~ Figure S1). While bootstrap and SH-aLRT values provided high support to our inferred species trees (~~Fig.~~ Figure 1), we found evidence for considerable discordance across individual UCE phylogenies. The five shortest branches in the concatenated tree had a site concordance factor (sCF) of less than 50%, suggesting that alternate resolutions of the quartet had equivocal support (~~Fig.~~ Figure S2). Gene concordance factors (gCF) for each branch in the species tree were on aggregate much higher, with all but four branches supported by almost every gene tree in the analysis and with the lowest values likely being driven by a several short internal branches (~~Fig.~~ Figure S2). This pattern was recapitulated using a quartet-based summary method (Figs. S1 and S3). At the two most discordant nodes (E and J in ~~Fig.~~ Figure 1), the recovered topology was supported by approximately one third of all gene trees.

We estimated divergence times for the inferred concatenated phylogeny (~~Fig.~~ Figure 1; Table S2) using four fossil calibration points (Table S3). The murid and cricetid groups had an estimated divergence time of 22.66 Ma (node A in ~~Fig.~~ Figure 1) followed by the Murinae and the Gerbillinae at 21.34 Ma (B), albeit with wide confidence intervals (CI) in both cases. The core Murinae (C) *sensu* Steppan et al. (2005) are inferred to have arisen 13.11 Ma (CI: 11.42 – 15.10).

Hydromyini then split off at 12.15 Ma (D, CI: 11.10 – 13.51) followed by Otomyini and Arvicanthini at 11.70 Ma (E, fossil calibration from Kimura, et al 2015). The remaining Murine tribes evolved in rapid succession, with Apodemini diverging from Murini and Praomyini at 10.84 Ma (F). Murini and Praomyini then split at 10.19 Ma (H). The two *Rattus* species in our dataset were inferred to have diverged 2.01 Ma (Q, CI: 1.26 – 2.30). Although congruent with previous works (Lecompte, et al. 2008; Steppan and Schenk 2017), this dated UCE phylogeny provides context on the evolutionary timescale upon which we next describe the genomic landscape of phylogenetic discordance across a collection of murine genomes.

The landscape of phylogenetic discordance along murine genomes

We analyzed genome-wide phylogenetic histories of six recently sequenced murine rodent genomes and the *M. musculus* reference genome spanning approximately 12 million years of divergence (see ~~Fig.~~ Figure 1). Using the *M. musculus* coordinate system, we partitioned and aligned 263,389 non-overlapping 10 kb windows from these seven species (Table S1). After filtering windows in repetitive regions or with low phylogenetic signal, we recovered 163,765 trees with an average of 616 informative sites per window (~~Fig.~~ Figure S4).

Phylogenetic discordance was pervasive within and between chromosomes. We inferred 597 of the 945 possible unique rooted topologies among six species (when specifying *R. soricoides* as the outgroup) across all chromosomes. The number of unique topologies per chromosome ranged from 75 to 218 (mean = 141). However, just four different topologies were ranked in the top three per chromosome. (Fig 2A; File S1) and only nine trees were present at a frequency above 1%. Among these, the top three topologies only differed in the ordering of the clade containing *Hylomyscus alleni, Mastomys natalensis,* and *Praomys delectorum* (HMP clade). This clade also showed the second lowest concordance in the species tree inferred from UCEs (~~Fig.~~ Figure 1, node J). These three topologies comprise between 13-15% of all recovered topologies (~~Fig.~~ Figure 2). Interestingly, the least common of these three trees (13.1%) matched the topology recovered via concatenation of all coding regions and the species tree recovered from UCEs (~~Fig.~~ Figure 1). That is, the robustly inferred species tree did not match the evolutionary relationships inferred for over 85% of the genome.

While visual inspection revealed no clear partitioning of topological structures along chromosomes (*e.g.*, ~~Fig.~~ Figure 2C), we found that phylogenies were not randomly distributed across mouse chromosomes. Using the weighted Robinson-Foulds metric, we found that tree similarity between windows decayed logarithmically along chromosomes (~~Fig.~~ Figure 3A and B), and the distance at which tree similarity appeared random varied considerably among chromosomes ranging from 0.15 Megabases (Mb) on chromosome 17 to 141.29 Mb on the chromosome 2 (~~Fig.~~ Figure 3C, ~~Fig.~~ Figure S5). While chromosomes 2, 7, 9, and 11 were autosomal outliers with distances between windows to random-like trees exceeding 25 Mb, the average distance among all other autosomes was only 2.1 Mb. The rates at which phylogenetic similarity decayed tended to be inversely proportional to the distance at which two randomly drawn phylogenies lost similarity (~~Fig.~~ Figure 3D).

Next, we performed a pairwise alignment of the reference mouse and rat genomes to assess how large structural variations, such as inversions and translocations, may influence our inferences of phylogenetic relatedness along the genome. These species span the deepest divergence of the sample for which we assessed genome-wide discordance, so the level of large structural variation present among them should give us an idea of the amount of ancestral variation in our sample. The mouse and rat genomes were mostly co-linear for large, aligned chunks, with large translocations and inversions on mouse chromosomes 5, 8, 10, 13, and 16 (~~Fig.~~ Figure S6). We also observe large-scale inversions on chromosome 16. We found that, while most chromosomes were co-linear between mouse and rat, the average size of the 307,275 contiguously aligned chunks averages under 10 kb, with the average distance between aligned segments being between 2,380 bp on the mouse genome and 4,927 bp on the rat chromosome (~~Fig.~~ Figure S7). This pattern presents two major implications for our analyses. First, we could not transpose the coordinate system from mouse to rat with enough resolution to use genetic maps from rat. Second, most other structural variations in our sample appear likely to be small insertions of transposable elements (e.g., SINEs ~150-500 bp, LINEs ~4-7kb; Platt, et al. 2018) that should have a negligible effect on discordance analyses since our window size is much larger and we excluded windows that were made up of mostly repeats.

Discordance with recombination rate and other genomic features

Using markers from genetic crosses within *M. musculus* (Shifman, et al. 2006; Cox, et al. 2009) we examined whether regions with high recombination also showed more phylogenetic discordance over short genetic distances when compared to regions with low recombination. Specifically, we calculated recombination rates within 5 Mb windows (~~Fig.~~ Figure S8) and then measured tree similarity between the first and last 10 kb window (R^2 = 3.0e-9; p = 0.99; ~~Fig.~~ Figure 4A) and the rate at which tree similarity changes between the first 10 kb window and every other 10 kb window (R^2 = 0.003; p = 0.11; ~~Fig.~~ Figure 4B). Surprisingly, we found no relationship between tree similarity and recombination rates measured at this scale. However, we did observe a slight positive correlation between recombination rate and dissimilarity to the species tree when averaging wRF over all 10 kb window trees within a 5 Mb recombination window (R^2 = 0.05; p = 7.6e-8; ~~Fig.~~ Figure 4C). We also examined regions of the genome centered on recombination hotspots identified in *M. musculus* (Smagulova, et al. 2011) and found that these regions had significantly slower rates of decay in similarity over genomic distance compared to windows that were not centered on hotspots (p = 0.019; ~~Fig.~~ Figure 5A), and that they were also significantly more phylogenetically similar over short distances (p = 0.015; ~~Fig.~~ Figure 5B). Thus, when taken as a whole, we found that regions of higher recombination rates in house mice did not show more local phylogenetic discordance per se but did tend to show more discordance relative to the genome-wide species tree.

Evolutionary relationships around certain conserved genomic features may also be shaped by locally reduced effective population sizes due to a history of pervasive linked negative or positive selection. To test for this, we measured tree similarity in 10 kb windows around all

annotated protein-coding genes, ultra-conserved elements (UCEs), and protein-coding genes identified as evolving rapidly (*i.e.*, significantly elevated d_N/d_S) due to positive directional selection and compared these patterns relative to chromosome-wide trends (i.e., windows without annotated features). In general, UCEs showed more local phylogenetic similarity among adjacent windows (i.e., less discordance) than regions surrounding recombination hotspots (p = 2.42e-12), coding genes (p = 4.65e-14), rapidly evolving coding genes (p = 1.56e-6), and windows that did not include any of these features (p = 5.02e-14; ~~Fig.~~ Figure 5A). In contrast, protein-coding genes (including rapidly evolving genes) were indistinguishable from background rates of discordance observed in windows without annotated genomic features (~~Fig.~~ Figure 5A). Likewise, UCEs were also much more similar to the overall species tree when compared to any other feature (~~Fig.~~ Figure 5B). Unlike our test of local discordance, protein-coding genes also showed less species tree discordance than windows containing no features or recombination hotspots, but the effect was much less pronounced than observed at UCEs.

Consequences of tree misspecification on analyses of molecular evolution

Next, we examined how phylogenetic discordance influenced inferences on the evolution of protein-coding sequences. Among a set of 22,261 *M. musculus* protein-coding transcripts, the average distance between the start and end of the coding sequence was 37.02 kb, or roughly 4 non-overlapping 10 kb windows. At this distance, tree similarity is predicted to diminish considerably (*e.g.*, by 0.10 wRF units), such that the phylogenetic history of individual genes may often contain some phylogenetic discordance (Mendes and Hahn 2016; Mendes, et al. 2019). We also found that out of the 67,566 times the coding sequence in a gene overlapped with a 10 kb window, the inferred topology of the gene tree exactly matched the topology of the corresponding window tree only 11% of the time. Thus, the common practice of inferring gene trees on concatenated coding exons from a single transcript is still likely averaging over multiple possible albeit correlated histories.

Finally, we tested how tree misspecification might impact standard d_N/d_S based phylogenetic analyses for positive directional selection. Specifically, we used the still common practice of assuming a single species tree for all genes and compared that to using individually inferred gene trees in three common statistical tests for positive selection: PAML's M1a vs. M2a test (Yang 2007), HyPhy's BUSTED test (Murrell, et al. 2015), and HyPhy's aBSREL test (Smith, Wertheim, et al. 2015). We found evidence that tree misspecification likely induces both false positive (type I) and false negative (type II) errors. For example, many genes were inferred as having experienced positive directional selection when using a single species tree, but not when using local gene trees and vice versa (~~Fig.~~ Figure 6). Assuming the locally inferred gene tree is more accurate than the single tree inferred from concatenation of all gene sequences, this resulted in varying rates and types of error (Table 1). For BUSTED, we observe that 28% of genes inferred as having evolved under positive directional selection when using the gene tree were not inferred when using the concatenated species tree (likely false negatives). The opposite was true for M1a vs. M2a, where, among genes showing inconsistent evidence for positive selection across the two scenarios, 76% do so when using the concatenated species tree but not individual gene trees (likely

false positives). In general, genes found to be evolving under positive selection using both tree types tended to be more concordant with the species tree than those that had evidence for positive selection either using only the concatenated tree or the gene tree (~~Fig.~~ Figure 6).

Discussion

Phylogenies provide insight into the relationships of species and serve as a framework for asking questions about molecular and trait evolution. However, phylogenetic histories can vary extensively across regions of a genome, and evolutionary relationships between species may not often be well represented by a single representative species-level phylogeny. Here, we combine the resources of the house mouse (*Mus musculus*) with new and recently published (Kumon et al. 2021) genomes from seven species to understand the systematics of murine rodents and causes and consequences of phylogenetic discordance along murine genomes. These new analyses help to place this important model system in a stronger evolutionary context and begin to fill the gap in genome sampling of murine rodents, which, despite their exceptional morphological and ecological diversity and species richness, have had relatively few whole genomes sequenced. They further provide us with the resources to study the landscape of phylogenetic discordance across the genome, understand how recombination and natural selection shape phylogenetic histories, and evaluate how assuming a single evolutionary history can compromise the study of molecular evolution in an important biomedical model system.

Phylogenomic relationships of murine rodent lineages from conserved genomic regions

The extraordinary species richness of murine rodents complicates phylogenetic analyses because of the resources required to sample, sequence, and analyze such widely distributed taxa. Earlier work either attempted to resolve specific groups such as *Mus* (Lundrigan, et al. 2002; Suzuki, et al. 2004) and *Apodemus* (Serizawa, et al. 2000; Liu, et al. 2004), or to uncover broader relationships across the subfamily (Martin, et al. 2000; Steppan, et al. 2005) based on a few genetic markers. Lecompte et al. (2008) provided one of the earliest well-supported phylogenetic reconstructions from across Murinae and the tribal classifications they proposed remain generally supported. More recent work has increased the number of taxa sampled, both for analyses of Murinae specifically (Pagès, et al. 2016) and for their placement within Muridae and Muroidea (Schenk, et al. 2013; Steppan and Schenk 2017; Rowe, et al. 2019), but the number of loci used for phylogenetic inference remained limited. Other recent studies have greatly expanded the number of loci used for phylogenetic inference (Mikula, et al. 2021), including the use of 1,245 exons (Roycroft, et al. 2020) and 1,360 exons (Roycroft, et al. 2021), but have focused on specific tribes within Murinae.

Our inferred species tree based on 2,632 UCEs from 18 species across the radiation (~~Fig.~~ Figure 1) is consistent with previous studies (Lecompte, et al. 2008; Steppan and Schenk 2017; Aghova, et al. 2018). Branch support was uniformly high, and gene trees unambiguously support the tribal classification of Lecompte, et al. (2008). However, four shorter branches show more

substantial gene tree discordance (~~Fig.~~ Figure 1, branches D, E, H, and J), with two recovered clades (E and J) being supported by less than half of all gene trees. We also estimated divergence times on our inferred species tree using four fossil calibration points (Table S3), recovering times that are roughly consistent with the relatively young estimates found by (Steppan and Schenk 2017) (see Supplement). This dated species tree provides an evolutionary timescale to evaluate the genomic landscape of phylogenetic discordance across ~12 my of murine evolution.

The genomic landscape of phylogenetic discordance

Limiting the number and nature of the loci used to resolve species relationships is often useful to get an initial picture of the history of speciation across many taxa. However, such targeted approaches may fail to capture the degree of discordance driven by incomplete lineage sorting and introgression (Alexander, et al. 2017; Chan, et al. 2020; Vanderpool, et al. 2020; Alda, et al. 2021). Our results highlight the limitations of a reduced marker-based approach and the general relationships between phylogenetic patterns and functional attributes of the genome in several interesting ways. Using the house mouse genome annotation, we found that the species tree inferred from only genes or UCEs did not match evolutionary relationships inferred for over 85% of the genome. Although similar frequencies were observed among these three most common trees (~~Fig.~~ Figure 2), the topology robustly inferred from genes or UCEs was not that common overall and only the third most frequent topology among 10 kb windows genome-wide. This result was driven mainly by discordance among three more closely related (Praomyini) species sampled for this study, which had nodes with low concordance in the UCE species tree (Fig 1, node J). In the window analysis, each alternate topology of this clade occurred at a frequency of ~14% while the rest of the topology remained consistent with the species tree (~~Fig.~~ Figure 2), indicating that the alternate topologies are caused by high levels of ILS at these nodes. Increased discordance at unresolved nodes is a common feature of phylogenomic datasets. These patterns illustrate how extensive discordance can arise even in a small sample of species and underscores that a single inferred species tree often may not capture the history of individual regions of the genome.

Given the fundamental role that recombination should play in shaping patterns of genetic variation within genomes, it is reasonable to assume that patterns of ILS should be broadly shaped by local recombination rate. We did not observe a clear relationship between local recombination rates in mice (*M. musculus*) and the degree of local phylogenetic discordance (i.e., phylogenetic similarity over 5 Mb intervals). However, we did find that regions of high recombination rate tended to be more discordant with the inferred species tree, in line with findings in other mammals (Pease and Hahn 2013; Foley, et al. 2023; Rivas-Gonzalez, et al. 2023) and *Drosophila* (Pease and Hahn 2013). Recombination rates evolve fairly rapidly both within (Kong, et al. 2002; Cox, et al. 2009; Stapley, et al. 2017) and between mammalian species (Jensen-Seaman, et al. 2004; Ptak, et al. 2005; Stevison, et al. 2016; Stapley, et al. 2017) due, in part, to the high turnover of hotspots due to the changing landscape of binding sites for PRDM9 (Baudat, et al. 2010; Singhal, et al. 2015). Similar to findings in great apes (Hobolth, et al. 2007), our results suggest that high-resolution genetic maps from a single species provide some weak predictive value for

understanding broader patterns of species tree discordance. However, these limited estimates may not be predictive of finer-scale patterns in a sample spanning over 12 million years of mammalian evolution (but see Foley, et al. 2023). Overall, the evolution of recombination landscapes across closely related species remains an important empirical question in evolutionary genetics (Dapper and Payseur 2017), especially as the generation of chromosome-scale genome assemblies continues to greatly outpace estimates of patterns of recombination within those genomes.

One source of evolution in the recombination map may be changes in synteny. Our reference-guided analyses assume collinearity between *Mus* and the other lineages we are comparing (*i.e.*, no karyotype variation), at least at the window-based scale we are comparing variation. Structural variation, including substantial variation in chromosome numbers, is likely to be widespread in rodents (Stanyon, et al. 1999; Yalcin, et al. 2011; Romanenko, et al. 2012; Keane, et al. 2014) and has the potential to skew our results when comparing tree similarity between regions of the genome using multiple species. Generating chromosome-scale assemblies for many non-*Mus* and *Rattus* species may prove limiting given that most tissue resources for this group are derived from natural history collections that often lack high molecular weight DNA. Nonetheless, whole genome alignments between mouse and rat indicate high degrees of chromosomal synteny and co-linearity (Fig S6), suggesting that many regions will be colinear in our sample.

Natural selection reduces the effective population size (N_e) of genomic regions through genetic hitchhiking of variation linked to the fixation of positively selected mutations (i.e., selective sweeps; Smith and Haigh 1974; Kaplan, et al. 1989) and the purging of deleterious mutations (i.e., background selection; Charlesworth, et al. 1993; Hudson and Kaplan 1995). Thus, variation in parameters dependent on N_e – such as standing levels of nucleotide variation and patterns of incomplete lineage sorting – should be reduced by linkage to functional elements subject to selection. Consistent with this, we observed the lowest rates of local discordance (~~Fig.~~ Figure 5A) and overall gene tree/species tree discordance (~~Fig.~~ Figure 5B) near UCEs when compared to all other genomic features we studied. These results suggest that a history of recurrent purifying selection on UCEs (Katzman, et al. 2007) strongly reduces patterns of discordance through a persistent local reduction in N_e. In contrast, protein coding genes showed rates of local discordance that were similar to background levels, even when considering genes rapidly evolving due to positive directional selection (~~Fig.~~ Figure 5A). However, both classes of genes did show less species tree discordance than background consistent with previous results (Scally, et al. 2012; Rivas-Gonzalez, et al. 2023), but this effect was much weaker than as observed at UCEs (~~Fig.~~ Figure 5B). Collectively, these data suggest that the frequency and strength of selection plays an important role in structuring patterns of incomplete lineage sorting across the genome over deeper evolutionary timescales.

One practical consequence of this is that phylogenetic inferences based on UCE markers would seem less prone to discordance and may provide cleaner estimates of species tree history than randomly chosen or protein-coding regions. Indeed, windows centered on UCEs have a higher degree of similarity to the species tree than other genomic features (i.e., 17% concordance with the species tree, versus 13% genome-wide or 15% for protein-coding genes). However, it is worth

noting that UCEs are also more likely to provide a potentially misleading underestimate of genome-wide levels of discordance. Given this relationship, species tree inferences based on UCEs should likely not, for example, be extended to related population genetic parameters of interest (*e.g.*, ancestral population sizes, estimates population genetic diversity), and could mislead the reconstruction of trait evolution across phylogenies (Avise and Robinson 2008; Hahn and Nakhleh 2016; Mendes, et al. 2018; Hibbins, et al. 2023). Finally, despite the relative ease of generating UCE data, such markers are likely unsuitable for genetic inferences within populations given the pervasive effects of linked selection.

Discordance and Molecular Evolution

We also found that the choice of tree topology drastically affects the results from various common tests for positive selection. Previous studies have used simulations to show that tree misspecification can lead to incorrect placement of substitutions on branches, possibly leading to spurious results for tests of positive directional selection within empirical datasets (Mendes and Hahn 2016). Here, we use empirical data in mice to show that these errors result in false positive (detected signal for selection only when using the gene tree) and false negative results (detected signal for selection only when using the species tree).

For each of the three selection tests run, HyPhy's BUSTED and aBSREL and PAML's M1a vs. M2a, some genes showed evidence of positive selection whether the species tree or gene tree was used. In contrast, many other genes had signatures of positive selection restricted only to a single tree. The genes unique to the type of tree used were often discordant with the species tree while the genes that showed evidence of positive selection regardless of the tree used had levels of discordance comparable to all genes (85%, ~~Fig.~~ Figure 6, numbers in parentheses). This suggests that mis-mapping substitutions by supplying these tests with the wrong tree (*i.e.*, the species tree when gene trees are discordant) can lead to inflated false positive and false negative rates when inferring genes under positive selection. The magnitude and direction of these biases were dependent on the underlying model. So-called branch-site models that allow substitution rates to vary among both branches and codon sites, such as HyPhy's BUSTED and aBSREL models, resulted in more genes inferred with evidence for positive selection when using the inferred gene tree (*i.e.*, the correct tree, assuming no errors in gene tree reconstruction). This means that using a single species tree for these tests reduces the power to detect positive selection. On the other hand, models that only allow rates to vary among sites, such as PAML's M1a vs. M2a test, showed an increase in the number of putative false positives inferred when using the wrong tree. That is, tree mis-specification results in spurious increases in d_N/d_S that mimics positive directional selection.

These results have wide-ranging implications for phylogenetics and comparative genomic analysis. First, it is imperative that when testing a specific locus for positive selection, discordance among loci must be accounted for. This is most easily achieved by simply using the gene tree (or other locus type) as input to the test for selection (Good, et al. 2013; Mendes and Hahn 2016; Roycroft, et al. 2021). However, as Mendes and Hahn (2016) pointed out, this may not completely mask the effects of discordance on substitution rates, as sites within a single gene may still have

evolved under different histories because of within-gene recombination. Indeed, we found that tree similarity diminished at scales that were less than the average genomic distance between the beginning and end of a coding sequence in mice (~37 kb in this data set). Nevertheless, starting with an inferred gene tree is advisable whenever possible, followed by a secondary analysis of evidence for within-gene variation in phylogenetic history.

Our results also imply that studies of molecular evolution may benefit from approaches that reduce genome-wide levels of discordance, such as through *post hoc* pruning of species that disproportionately contribute to unresolved nodes.

Incorporating discordance into a comparative framework is not trivial and many comparative genomic methods assume a single species tree that test for changes in substitution rates in a phylogeny (Pollard, et al. 2010; Hu, et al. 2019; Partha, et al. 2019). Even methods that allow the use of different trees for different loci (like PAML and HyPhy) are still commonly applied with a single species tree across loci (Carbone, et al. 2014; Foote, et al. 2015; van der Valk, et al. 2021; Treaster, et al. 2023). While we used the simplifying assumption that the results from the gene tree are more likely to be correct, this may not always be the case given that errors can also occur during gene tree inference. Still, our results confirm that the use of a single tree for all loci for such tests that rely on accurate estimation of substitution rates are likely to lead to both inaccurate inferences of positive selection. We strongly encourage the use of individual gene trees for such analyses.

Conclusions

Murine rodents as a study system allow us to use the high-quality *M. musculus* genome to examine fine-scale patterns and effects of phylogenetic discordance along chromosomes. Our analysis reveals how discordance varies with genome biology across evolutionary timescales, as well as the limits of inference inherent to extrapolating information from a single model system to a phylogenetic sample. We also demonstrate how phylogenetic discordance can mislead common tests for selection if only a single species tree is used. Overall, our results emphasize that progress in comparative genomics requires a detailed understanding of the heterogeneous biological signals in phylogenomic datasets. Through these results, we can better understand the complexities of phylogenomic datasets and the effects of underlying biological processes on large-scale analyses and ensure that steps are taken to accommodate and study these details.

Materials & Methods

Sample collection and assembly

We collected genomes from 16 murine species and ~~2~~two other rodents from several sources, including NCBI and several recently sequenced in Kumon, et al. (2021) (see Table ~~1~~S1 for full list of samples and sources). We also report the ~~sampling~~genome of *Otomys typus* (FMNH 230007) from Ethiopia in 2015. While DNA extraction and sequencing on the 10x Genomics platform for *O. typus* is the same as described in (Kumon, et al. 2021), the library quality for this sample was

too low for chromosome level assembly. Here, we instead assembled it into scaffolds with the express purpose of obtaining UCEs for phylogenetic analysis. Adapters and low-quality bases were trimmed from the reads using illumiprocessor (Faircloth 2013), which makes use of functions from trimmomatic using the default parameters (Bolger, et al. 2014). All cleaned reads were de novo assembled using ABySS 2.3.1 (Jackman, et al. 2017) with a Bloom filter (Bloom 1970) de Bruijn graph. The final *O. typus* scaffold assembly was 2.14GB (N50=9,211; L50=64,014; E-size=12,790).

In parallel, for six of these species (see ~~Fig. ~~Figure 1; Table ~~1; Fig. ~~Figure ~~1~~S1), we generated reference-based pseudo-assemblies with iterative mapping using an updated version pseudo-it v3.1.1 (Sarver, et al. 2017) that incorporates insertion-deletion variation to minimize reference bias in our genome-wide phylogenetic analyses and to maintain collinearity between assemblies (https://github.com/goodest-goodlab/pseudo-it). We used the *Mus musculus* (mm10) genome as the reference for our pseudo-assembly approach. Briefly, pseudo-it maps reads from each sample to the reference genome with BWA (Li 2013), calls variants with GATK HaplotypeCaller (Poplin, et al. 2018), and filters SNPs and indels and generates a consensus assembly with bcftools (Danecek, et al. 2021). The process is repeated, each time using the previous iteration's consensus assembly as the new reference genome to which reads are mapped. In total, we did three iterations of mapping for each sample.

Ultraconserved element (UCE) retrieval and alignment

~~To~~We first set out to reconstruct a ~~broad~~ phylogeny of sequenced murine rodents~~, we~~ to provide both a useful resource for future comparative genomic studies within this important group as well as a time-calibrated phylogeny to frame an in-depth analysis of phylogenetic discordance across a subset of murine whole genomes (see below). We combined our seven recently sequenced genomes with nine publicly available ~~genomes from other Old World mice and rats (subfamily Murinae)~~murine genomes as well as the genomes of two non-murine rodents, the great gerbil (*Rhombomys opimus*; (Nilsson, et al. 2020) and the Siberian hamster (*Phodopus sungorus*; (Moore, et al. 2022) as outgroups. We extracted UCEs from each species, plus 1000 flanking bases from each side of the element using the protocols for harvesting loci from genomes and the *M. musculus* UCE probe set provided with phyluce v1.7.1 (Faircloth, et al. 2012; Faircloth 2016). In total, we recovered 2,632 unique UCE loci, though not all UCE loci were found in all taxa (Table ~~1~~S1).

We brought the extracted UCE sequences for each species into a consistent orientation using MAFFT v7 (Katoh and Standley 2013) and then aligned them using FSA (Bradley, et al. 2009) with the default settings. We trimmed UCE alignments with TrimAl (Capella-Gutierrez, et al. 2009) with a gap threshold of 0.5 and otherwise default parameters. We performed alignment quality checks using AMAS (Borowiec 2016). We processed all alignments in parallel with GNU Parallel (Tange 2018).

Species tree reconstruction from UCEs

We constructed a species-level rodent phylogeny with two approaches. First, using the alignments of all UCEs found in four or more taxa (2,632), we reconstructed a maximum-likelihood (ML) species tree with IQ-TREE v2.2.1 (Minh, Schmidt, et al. 2020). Each UCE alignment was concatenated and partitioned (Chernomor, et al. 2016) such that optimal substitution models were inferred for individual UCE loci with ModelFinder (Kalyaanamoorthy, et al. 2017). We also reconstructed individual gene trees for each UCE alignment. For all IQ-TREE runs (concatenated or individual loci), we assessed branch support with ultrafast bootstrap approximation (UFBoot) (Hoang, et al. 2018) and the corrected approximate likelihood ratio test (SH-aLRT) (Guindon, et al. 2010). We collapsed branches in each UCE tree exhibiting less than 10% approximated bootstrap support using the nw_ed function from Newick Utilities (Junier and Zdobnov 2010). We used these trees as input to the quartet summary method ASTRAL-III v5.7.8 (Zhang, et al. 2018) to infer a species tree. We generated visualizations of phylogenies with R v4.1.1 (R Core Team 2021) using phytools v1.9-16 (Revell 2012) and the ggtree package v3.14 (Yu, et al. 2017; Yu 2020) and its imported functions from ape v5.0 (Paradis and Schliep 2019) and treeio v1.16.2 (Wang, et al. 2020).

We then used two methods to assess phylogenetic discordance across the reconstructed species tree. First, we calculated site and gene concordance factors (sCF and gCF) with IQ-TREE 2 (Minh, Hahn, et al. 2020; Minh, Schmidt, et al. 2020) to assess levels of phylogenetic discordance between the inferred UCE trees and the concatenated species tree. gCF is calculated for each branch in the species tree as the proportion of UCE trees in which that branch also appears (Baum 2007). sCF represents the proportion of alignment sites concordant with a given species tree branch in a randomized subset of quartets of taxa (Minh, Hahn, et al. 2020). (Minh, Hahn, et al. 2020). We visualized gCF and sCF (Lanfear 2018) for each branch in each species tree using methods in R v4.3.0 (Lanfear 2018; R Core Team 2021). Next, we used PhyParts (Smith, Moore, et al. 2015) to identify topological conflict between the UCE trees and the species tree from ASTRAL-III. For this analysis, we rooted all trees with *Phodopus sungorus* as the outgroup using the nw_reroot function in the Newick Utilities (Junier and Zdobnov 2010) package and excluded 204 UCE trees that did not contain the outgroup.

Divergence time estimation

We used IQ-TREE 2's (Minh, Schmidt, et al. 2020) implementation of least square dating to estimate branch lengths of our species trees in units of absolute time (To, et al. 2016). To improve divergence-time estimation, we used SortaDate (Smith, et al. 2018) to identify a set of 100 UCE loci that exhibit highly clocklike behavior and minimized topological conflict with the concatenated species tree. We applied node age calibrations (Table 2) from Schenk et al. (2013) and Steppan and Schenk (2017), which in turn were sourced from fossil calibrations described on Paleobiology Database (2011). As *Rattus* is paraphyletic, the maximum age is taken from the earliest crown group fossil on Paleobiology Database (2011). In contrast, the estimated *Rattus* node age from Schenk et al (2013) was used as the minimum age. Branch lengths were resampled 100 times to produce confidence intervals. To return a single solution, least square dating typically

~~requires that one calibration be fixed and not a range. We selected one calibration node (here, the branch leading to Murinae) and estimated dates across the tree when this node is set to its minimum, its maximum, and its midpoint ages. On the midpoint calibrated tree, we plot confidence intervals for each node representing the lowest minimum and highest maximum ages estimated across the three dating analyses.~~. To improve divergence-time estimation, we used SortaDate (Smith, et al. 2018) to identify a set of 100 UCE loci that exhibit highly clocklike behavior and minimized topological conflict with the concatenated species tree. We applied four node age calibrations (Table S3) as described in Kimura, et al. (2015) and Aghova, et al. (2018). The origin of core Murinae (Node E) was constrained to between 11.1 and 12.3 Ma, following Kimura, et al. (2015). Maximum ages were set for Otomyini+Arvicanthini (9.2 Ma, Kimura, et al. 2015), *Apodemus* (9.6 Ma, Daxner-Höck 2002), and *Mus* (8.0 Ma, Kimura, et al. 2013). Branch lengths were resampled 100 times to produce confidence intervals.

Genome window-based phylogenetic analysis

For the second part of our work, we wanted to quantitatively infer phylogenetic discordance across a subset of the murine genomes used to infer the species tree and relate that discordance to other features of the genome, such as recombination rate, proximity to genes, and rates of molecular evolution. To assess the distribution of phylogenetic discordance across ~~the~~ rodent ~~genome~~genomes, we limited subsequent analyses to *M. musculus* and the pseudo-assemblies (see above) of six of the genomes (*Mastomys natalensis*, *Hylomyscus alleni*, *Praomys delectorum*, *Rhabdomys dilectus*, *Grammomys dolichurus*, and *Rhynchomys soricoides*). *Otomys typus* was excluded from these analyses due to the inadequacy of the library outlined above.

We partitioned these genomes into 10 kilobase (kb) windows based on the coordinates in the reference *M. musculus* genome (mm10; Mouse Genome Sequencing, et al. 2002) using bedtools makewindows (Quinlan and Hall 2010). These coordinates were converted between the reference and the consensus sequence for each genome using liftOver (Hinrichs, et al. 2006). Note that this method assumes both collinearity of all genomes and similar karyotypes (see Discussion). We then removed windows from the subsequent analyses if (1) 50% or more of the window overlapped with repeat regions from the *M. musculus* reference RepeatMasker (Smit, et al. 2013-2015) file downloaded from the UCSC Genome Browser's table browser (Hinrichs, et al. 2006) or (2) 50% or more of the window contained missing data in ~~3~~three or more samples. Overlaps with repeat regions were determined with bedtools coverage (Quinlan and Hall 2010). We then aligned the 10kb windows with MAFFT (Katoh and Standley 2013), trimmed alignments with trimAl (Capella-Gutierrez, et al. 2009), and inferred phylogenies for each with IQ-TREE 2 (Minh, Schmidt, et al. 2020) which uses ModelFinder to determine the best substitution model for each window (Kalyaanamoorthy, et al. 2017).

To assess patterns of tree similarity between windows on the same chromosome, we used the weighted Robinson-Foulds (wRF) (Robinson and Foulds 1981; Böcker, et al. 2013) distance measure implemented in the phangorn library (Schliep 2011) in R (R Core Team 2021), which compares two trees by finding clades or splits present in one tree but not the other weighted by the

missing branch length in each tree for each mismatch and differences in branch length between the co-occurring branches in both trees (Robinson and Foulds 1979). Consequently, the resulting measure of wRF is in units of branch length (i.e., expected number of substitutions per site for maximum likelihood trees). We compared wRF between trees from windows on the same chromosome to characterize (1) heterogeneity in patterns discordance along the chromosome and (2) whether tree similarity is correlated with distance between windows. For the second question, we sampled every window on a chromosome at increasing distance (in 10kb windows) until the distribution of wRF scores for all pairs of windows at that distance was not significantly different (Wilcox test, $p > 0.01$) than that of a sample of 12,000 measures of wRF between randomly selected trees on different chromosomes. We selected 12,000 as the random sample size because it roughly matched the number of windows on the largest chromosome (chromosome 1, n = 12,113). We used Snakemake 7 (Mölder, et al. 2021) to compute window alignments and trees in parallel.

Whole genome alignment between mouse and rat

To assess how un-accounted for large-scale structural variation may impact our conclusions, we compared the reference mouse and rat genomes. We used minimap2 (Li 2018) to align the mouse (mm10) and rat (rnor6) (Gibbs, et al. 2004) genomes to assess the impact of structural variation that spans the divergence of our subset of species used ~~to~~ in the discordance analyses. We downloaded the rat reference genome (rnor6) from the UCSC genome browser and for both genomes removed the Y chromosome and all smaller unplaced scaffolds. We then used minimap2 in whole genome alignment mode (-x asm20) to generate a pairwise alignment file from which we calculated alignment segment sizes and the distances between alignment segments. We visualized the alignment as a dot plot using the pafr package in R (https://github.com/dwinter/pafr).

Recombination rate and functional annotation

We retrieved 10,205 genetic markers generated from a large heterogenous stock of outbred mice (Shifman, et al. 2006; Cox, et al. 2009) to assess whether phylogenetic discordance along chromosomes was correlated with mouse recombination rates. We converted the physical coordinates of these markers from build 37 (mm9) to build 38 (mm10) of the *M. musculus* genome using liftOver (Hinrichs, et al. 2006). We then partitioned the markers into 5Mb windows and estimated local recombination rates defined as the slope of the correlation between the location on the *M. musculus* genetic and physical maps for all markers in the window (White, et al. 2009; Kartje, et al. 2020). Within each 5Mb window, we calculated wRF distances between the first 10kb window and every other 10kb window.

We also compared the chromosome-wide wRF distances to those based on phylogenies from regions around several types of adjacent to genomic features. We retrieved coordinates from 25,753 protein coding genes annotated in *M. musculus* from Ensembl (release 99; Cunningham, et al. 2022), all 3,129 UCEs from the *M. musculus* UCE probe set provided with PHYLUCE

(Faircloth, et al. 2012; Faircloth 2016), and 9,865 recombination hotspots from Smagulova, et al. (2011). The recombination hotspot coordinates were converted between build 37 and build 38 using the liftOver tool (Hinrichs, et al. 2006). For each feature, the starting window was the 10kb window containing the feature's midpoint coordinate. We then calculated wRF between this window and all windows within 5Mb in either direction and for each chromosome compared the slope and wRF distance of windows adjacent to the feature with the same metrics for the whole chromosome. We compared distributions of these measures for each genomic feature with an ANOVA (aov(feature.measure ~ feature.label)) followed by Tukey's range test (TukeyHSD(anova.result)) to assess differences in means, as implemented in R v4.1.1 (R Core Team 2021).

Molecular evolution

To test how tree misspecification affects common model-based analyses of molecular evolution, we retrieved 22,261 coding sequences from *M. musculus* using the longest coding transcript of each gene. Coding coordinates from the *M. musculus* coding sequences were transposed to the new assemblies via liftOver (Hinrichs, et al. 2006) and sequences retrieved with bedtools getfasta (Quinlan and Hall 2010). We recovered 17,216 genes that were present in all ~~7~~seven species. Using MACSE (Ranwez, et al. 2018), we trimmed non-homologous regions from each ortholog using trimNonHomologousFragments, aligned the orthologs using alignSequences, and trimmed the aligned sequences with trimAlignment to remove unaligned flanking regions. Finally, we manually filtered the alignments using the following (non-mutually exclusive) criteria: 3,368 alignments were removed during filtering for gapped sites, 3,132 alignments had a premature stop codon in at least one species, 1,571 alignments had only ~~3~~three or fewer unique sequences among the ~~7~~seven species, and 78 alignments were shorter than 100 bp. After filtering, 12,559 total alignments for tree reconstruction and inference of selection.

We then used IQ-TREE 2 (Minh, Schmidt, et al. 2020) to reconstruct a single species tree from concatenation of all gene alignments, as well as gene-trees for each individual alignment. This species tree from coding regions matches the topologies of these species inferred by concatenation of UCEs in the previous section. Next we ran several tests that use both coding alignments and a tree to infer positive selection: PAML's M1a vs. M2a test (Yang 2007), HyPhy's aBSREL model (Smith, Wertheim, et al. 2015), and HyPhy's BUSTED model (Murrell, et al. 2015). We ran each test twice on each gene, once using the species tree derived from concatenated data, and once using the tree estimated for that gene. For the HyPhy models, no target branch was selected, meaning all branches in the input phylogeny were tested.

The end point ~~of each~~ of each of these three tests is a p-value, which lets us assess whether a model that allows for positively selected sites fits better than a model that does not. For M1a vs. M2a, we obtained the p-value manually by first performing a likelihood ratio test to determine genes under selection by calculating $2 * (lnl\ M1a - lnl\ M2a)$. The p-value of this likelihood ratio is then retrieved from a one-tailed chi-square distribution with ~~2~~two degrees of freedom (Yang 2007). For BUSTED and aBSREL, p-values are computed automatically during the test

using similar likelihood ratios. For the M1a vs. M2a and BUSTED tests, a single p-value is computed for each gene. P-values were adjusted by correcting for false discovery rates (Benjamini and Hochberg 1995; Yekutieli and Benjamini 1999) using the "fdr" method in the p.adjust() function in R (R Core Team 2021) and we categorized a gene as being positively selected if its adjusted p-value was < 0.01. For the aBSREL test, a p-value is generated for each branch in the input gene tree. aBSREL corrects for multiple testing internally across branches using the Holm-Bonferroni procedure (Holm 1979; Pond, et al. 2005). We further correct the p-values across genes with the Bonferroni method and classify a gene as having experienced positive selection if one or more branches has a p-value < 0.01 after all corrections. We used Snakemake 7 (Mölder, et al. 2021) to compute coding alignments, trees, and selection tests in parallel.

Data availability

For the six previously assembled genomes (see Table S1), all raw reads and assemblies are available as an NCBI BioProject (Accession Number PRJNA669840). The reads and assembly for *Otomys* typus, pseudo-assemblies for the six other new samples, and locus alignments (UCEs, genes, and genomic windows) are available on Dryad (https://doi.org/10.5061/dryad.866t1g1wq). All code and summary data for this project are deposited on github (https://github.com/gwct/murine-discordance).

Acknowledgments

We thank Jake Esselstyn and Kevin Rowe for helpful comments and discussion on the murine species tree and Matt Hahn and the Hahn lab for feedback on the manuscript. We also thank Brant Faircloth and Trevor Sless for advice on using phyluce. We are grateful for tissue samples provided by Chris Conroy at the Museum of Vertebrate Zoology, Berkeley, CA (MVZ) and Adam Ferguson at the Field Museum of Natural History, Chicago, IL (FMNH), and to the original collectors. This work was supported by the National Science Foundation (DEB-1754096 to J.M.G), the Eunice Kennedy Shriver National Institute of Child Health and Human Development of the National Institutes of Health (R01-HD094787 to J.M.G.). J.J.H. received financial support from the Cornell Center for Vertebrate Genomics. J.-S.-B. was supported by the University of Michigan Life Sciences Fellows Program and the Jean Wright Cohn Endowment Fund at the University of Michigan Museum of Zoology. Computations for species tree reconstruction were performed using the computer clusters and data storage resources of the University of California Riverside HPCC, which were funded by grants from NSF (MRI-2215705, MRI-1429826) and NIH (1S10OD016290-01A1), and the Cornell University Biotechnology Resource Center BioHPC (RRID:SCR_021757) with help from Qi Sun. Bioinformatic analyses for genomic discordance and selection tests were conducted using the University of Montana Griz Shared Computing Cluster supported by grants from the NSF (CC-2018112 and OAC-1925267,

J.M.G. co-PI). Any opinions, findings, and conclusions or recommendations expressed in this material are those of the authors and do not necessarily reflect the views of the NSF or the NIH.

Tables

Table 1: All taxa whose genomes were included in this study, the source of the assembly, and the assembly level of each genome. For the six samples used in the genome-wide discordance analyses (column 5, except for mm10), we also generated reference-based pseudo-assemblies using the mouse genome (mm10) as the reference.

Taxon	Assembly source	Assembly level	No. UCEs	Used in genome-wide discordance analyses
Apodemus speciosus	GenBank: GCA_002335545.1	Scaffolds	2336	
Apodemus sylvaticus	GenBank: GCA_001305905.1	Scaffolds	2510	
Arvicanthis niloticus	GenBank: GCA_011762505.1	Chromosomes	2563	
Grammomys dolichurus	Kumon et al., 2021: *de novo* assembled	Chromosomes	2395	*
Hylomyscus alleni	Kumon et al., 2021: *de novo* assembled	Chromosomes	2392	*
Mastomys natalensis	Kumon et al., 2021: *de novo* assembled	Chromosomes	2483	*
Mus caroli	GenBank: GCA_900094665.2	Chromosomes	2584	
Mus musculus	GenBank: GRCm38.p6/mm10	Chromosomes	2294	*
Mus pahari	GenBank: GCA_900095145.2	Chromosomes	2556	
Mus spretus	GenBank: GCA_001624865.1	Chromosomes	2578	
Otomys typus	This study: *de novo* assembled	Scaffolds	2627	
Phodopus sungorus	Moore et al., 2022: *de novo* assembled	Chromosomes	2633	
Praomys delectorum	Kumon et al., 2021: *de novo* assembled	Chromosomes	2549	*
Rattus norvegicus	GenBank: GCA_015227675.2	Chromosomes	2425	
Rattus rattus	GenBank: GCA_011064425.1	Chromosomes	2443	
Rhabdomys dilectus	Kumon et al., 2021: *de novo* assembled	Chromosomes	2546	*
Rhombomys opimus	GenBank: GCA_010120015.1	Scaffolds	2627	
Rhynchomys soricoides	Kumon et al., 2021: *de novo* assembled	Chromosomes	2570	*

Table 2: Prior node ages used in phylogenetic dating in millions of years before present.

Clade	Minimum Age	Maximum Age	Citation
Mus	5.3	7.2	Steppan and Schenk, 2017
Apodemus	5.3	7.2	Schenk et al., 2013
Rattus	2.4	3.6	Steppan and Schenk, 2017
Murinae	12.1	14.05	Schenk et al., 2013

Table 3: The most frequently recovered topologies across all 10kb windows. RS = *Rhyncomys soricoides*, GD = *Grammomys dolichurus*, RD = *Rhabdomys dilectus*, MM = *Mus musculus*, HA = *Hylomyscus alleni*, MN = *Mastomys natalensis*, PD = *Praomys delectorum*.

Rank	Topology	# of windows	Proportion of windows
1	(RS,((GD,RD),(MM,((HA,MN),PD))));	23864	0.146
2	(RS,((GD,RD),(MM,((HA,PD),MN))));	23836	0.146
3*	(RS,((GD,RD),(MM,(HA,(MN,PD)))));	21509	0.131
4	(RS,(MM,((GD,RD),((HA,MN),PD))));	14417	0.088
5	(RS,(MM,((GD,RD),((HA,PD),MN))));	14321	0.0874
6	(RS,(MM,((GD,RD),(HA,(MN,PD)))));	14044	0.0858
7	(RS,(((HA,PD),MN),(MM,(GD,RD))));	11723	0.0716
8	(RS,(((HA,MN),PD),(MM,(GD,RD))));	11308	0.0691

*The topology recovered from concatenation of genes or UCEs

Table 4: Summaries of phylogenies per chromosome.

Chromosome	# of unique topologies recovered
1	184
2	123
3	114
4	144
5	134
6	172
7	218
8	133
9	116
10	110
11	93
12	179
13	186
14	173

~~15~~	~~96~~
~~16~~	~~94~~
~~17~~	~~188~~
~~18~~	~~75~~
~~19~~	~~82~~
~~X~~	~~207~~

~~Table 5:.~~ Table 1. Rates and types of error when using ~~concatenated~~ a single species tree~~s~~ for gene-based selection tests~~.~~ (Assuming the gene tree topology is the correct topology).

Test	False positive rate	False negative rate
BUSTED	0.45%	28.10%
aBSREL	0.41%	10.60%
M1a vs. M2a	2.66%	3.20%

Figures

Figure 1

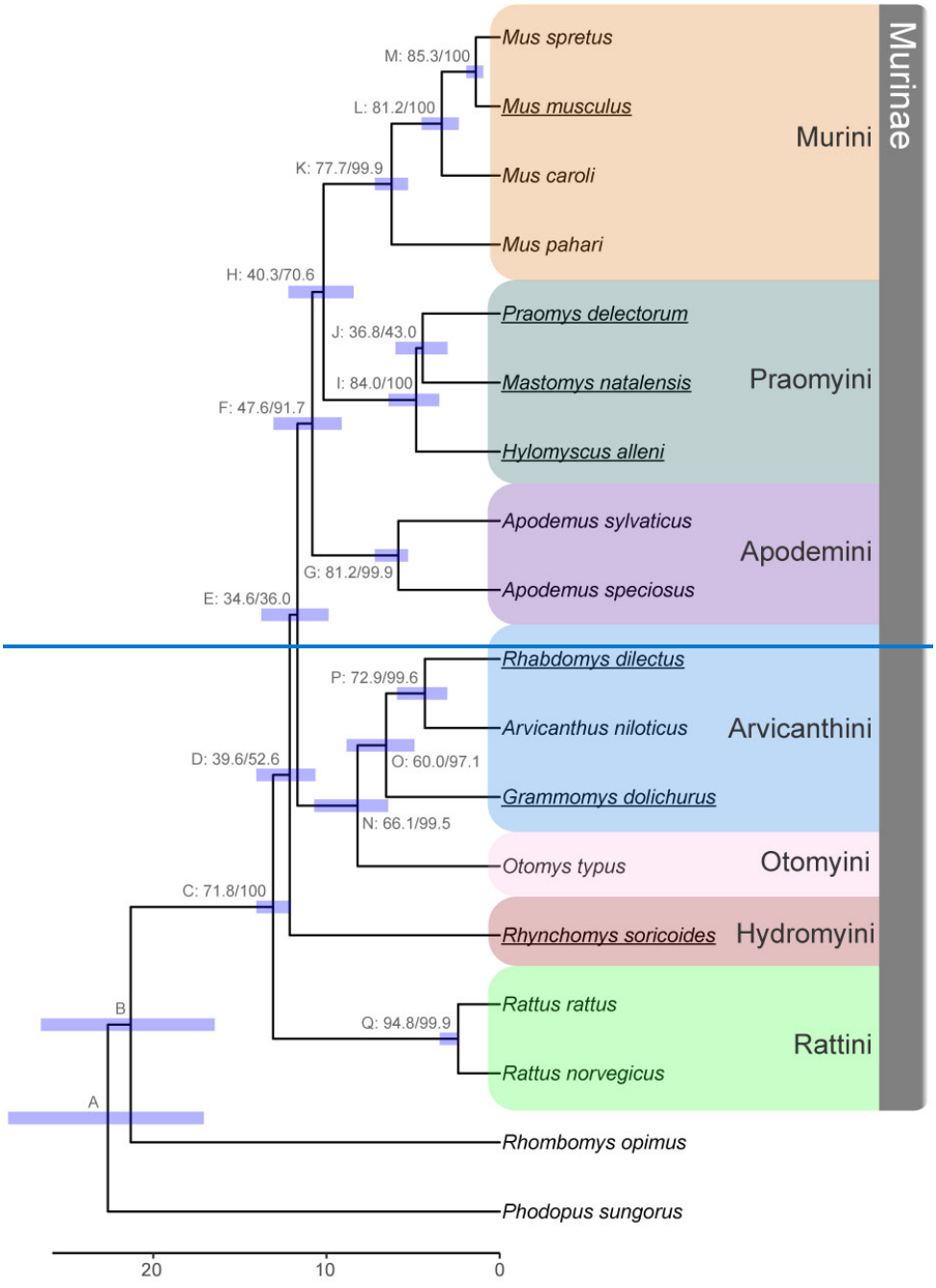

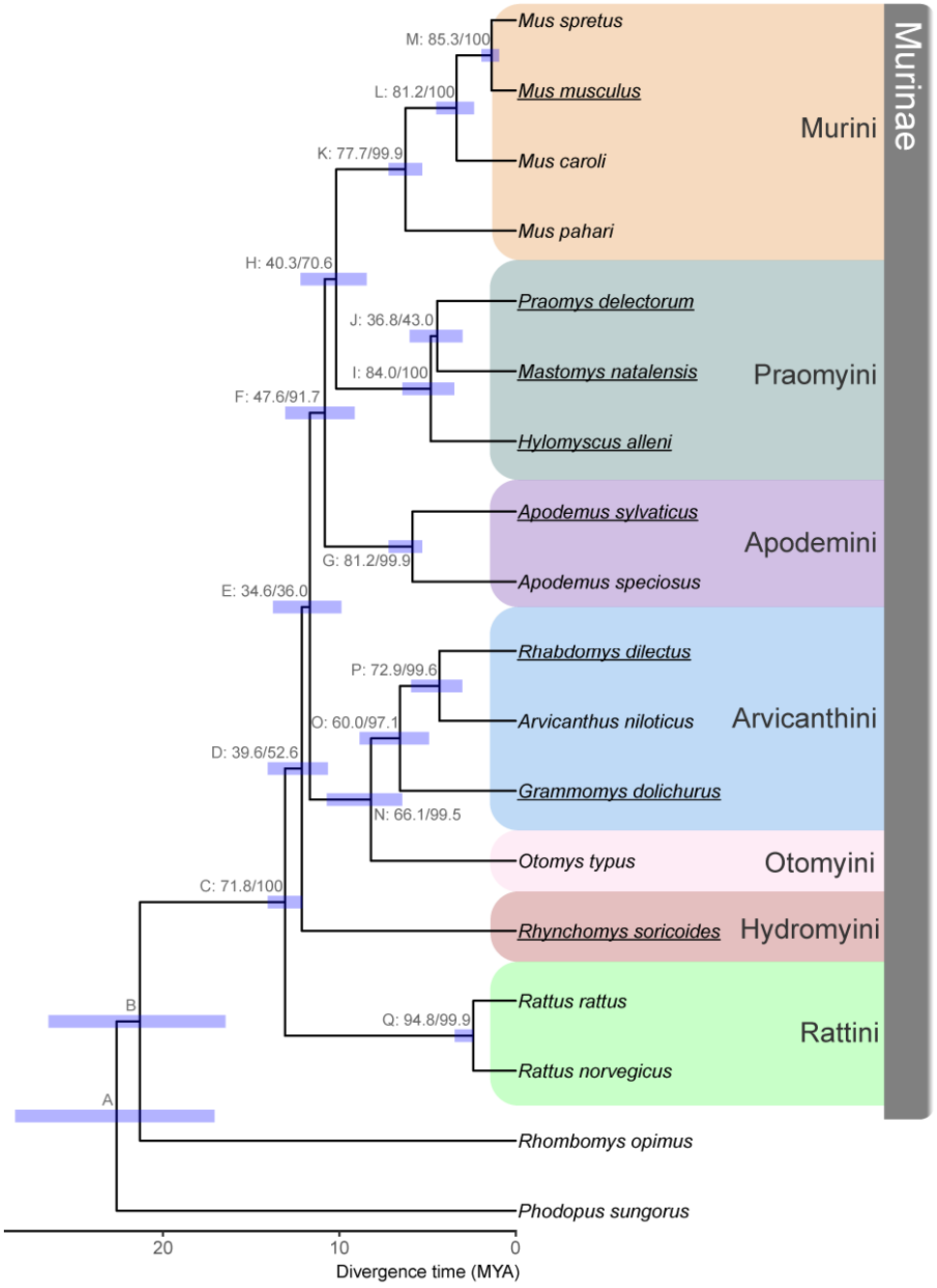

Figure 1~~.~~: Species trees inferred from concatenation of ultra-conserved elements (UCEs) from 18 rodent species. Internal nodes are labeled by a letter identifier referenced in the text and site and gene concordance factors (*i.e.*, Label: sCF/gCF) as well as a bar indicating the confidence interval for divergence time estimation. Ultrafast bootstrap/SH-aLRT values were all 100. Bottom scale represents time in millions of years before present. Fossil calibrations are described in Tables ~~2 and S2, with node C used as a fixed calibration point.~~S2 and S3. Tribes within sub-family Murinae are highlighted on the right following the classifications used by Lecompte, et al. (2008). Genomes used for the genome-wide phylogenetic discordance analyses are underlined.

Figure 2

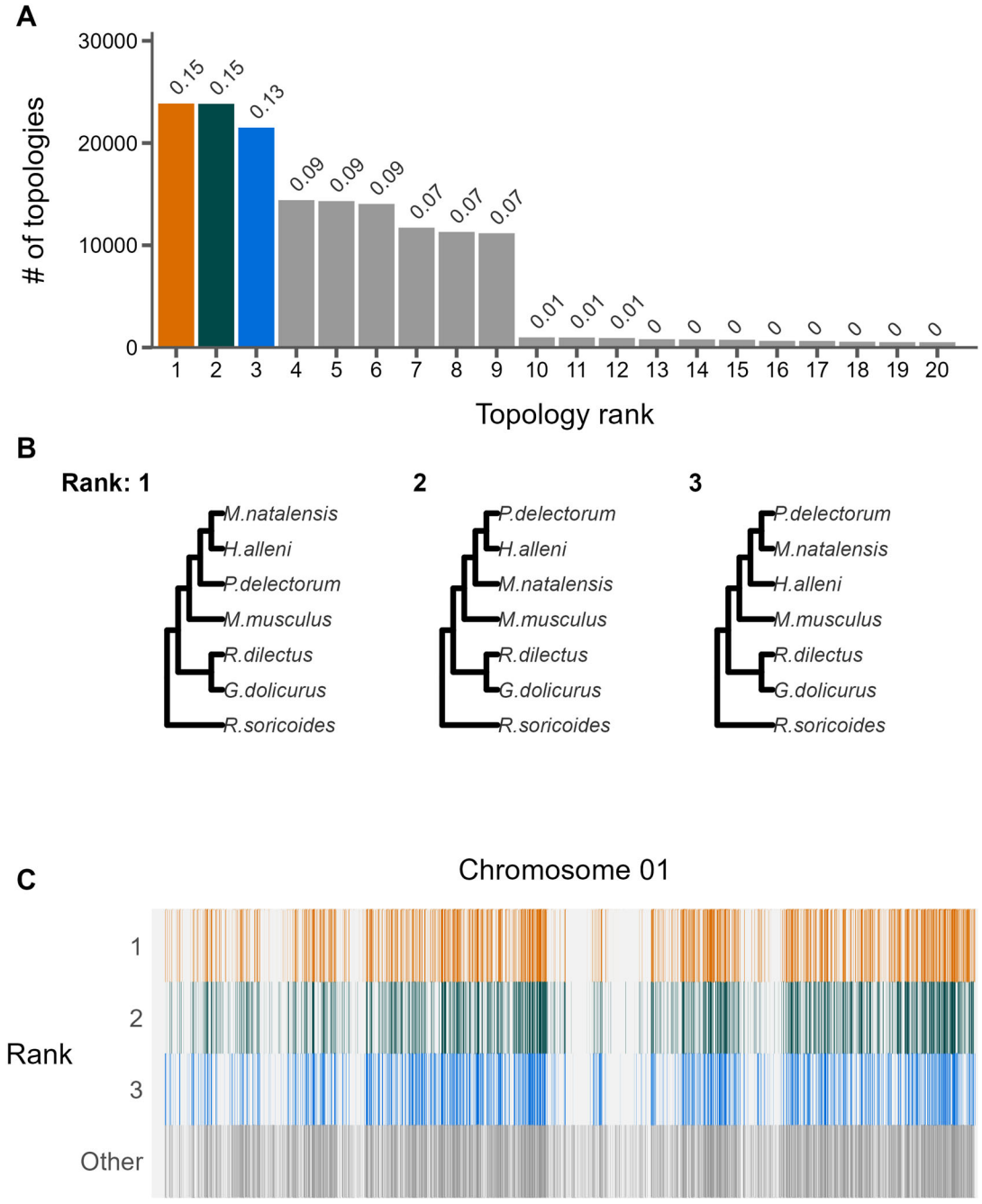

Figure 2. The landscape and profile of phylogenetic discordance across non-overlapping 10kb windows in murine genomes. A) Distribution of the 20 most frequent topologies recovered across all windows. Numbers above bars indicate proportion of each topology. B) The top three topologies recovered across all chromosomes 1. C) Distribution of the topologies recovered along

chromosome 1. The x-axis is scaled to the length of the chromosome and each vertical bar represents one 10kb window. The three most frequent topologies occupy the first three rows while all other topologies are shown in the bottom row. See Supplemental File S1 for individual chromosome plots.

Figure 3

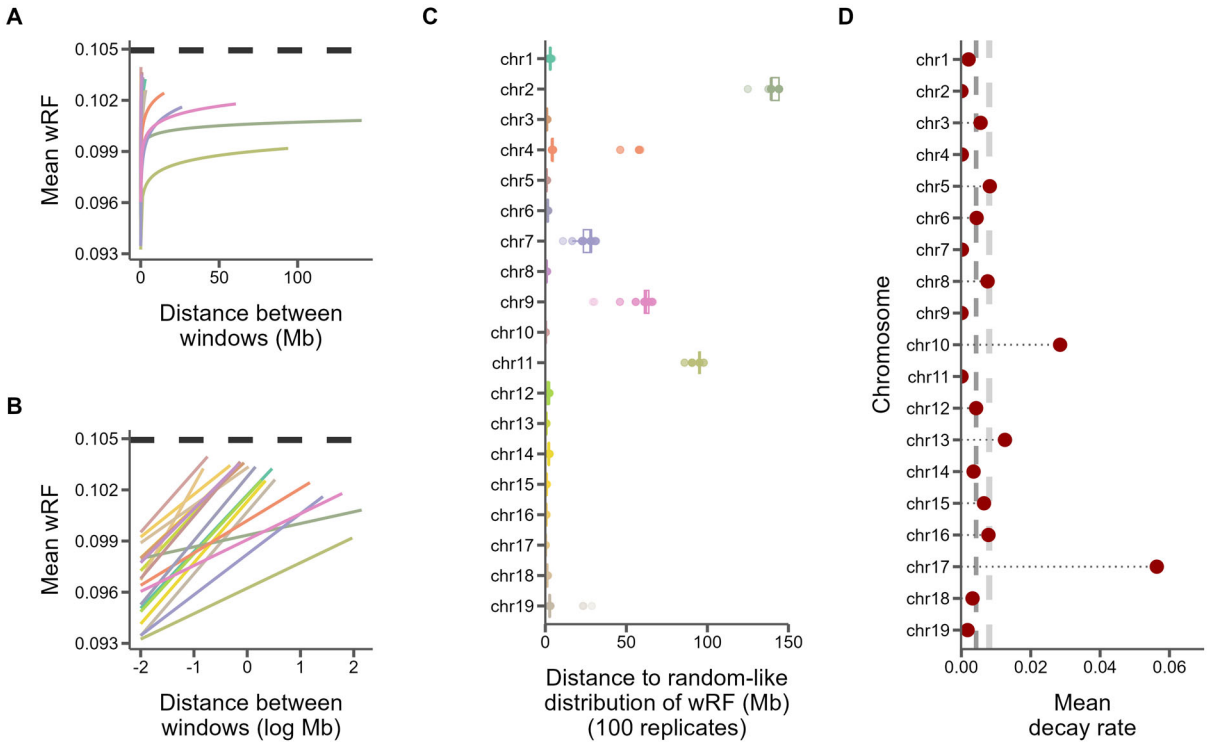

Figure 3~~:~~. Similarity between 10kb windows decays as genomic distance between windows increases. A) The log fit to the mean of distributions of weighted Robinson-Foulds distances between trees of windows at increasing genomic distance (10kb steps). Each line represents one chromosome. B) The same, but on a log scale with a linear fit. C) For every window on each chromosome, the genomic distance between windows at which tree distance becomes random for 100 replicates of random window selection. D) ~~The~~ Points represent the slopes of the correlation between genomic distance and tree distance (lines from panel B ~~represent~~), which is the rate at which tree similarity decays across the genome. Dark grey dashed line is median slope and light grey dashed line is mean.

Figure 4

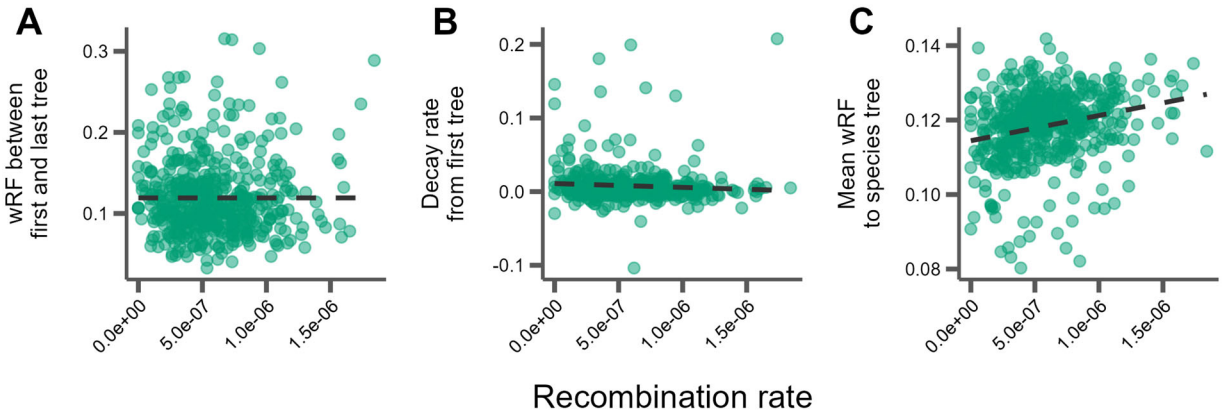

Figure 4~~:~~. Correlations between tree similarity and recombination rate in ~~5Mb~~5 Mb windows. A) Tree similarity as measured by the weighted Robinson-Foulds distance between the first and last ~~10kb~~10 kb windows within the ~~5Mb~~5 Mb window. B) The slopes of the linear correlation between the weighted Robinson-Foulds distances between the first ~~10kb~~10 kb window and every other ~~10kb~~10 kb window within a ~~5Mb~~5 Mb window represent the rate at which tree similarity decays over each ~~5Mb~~5 Mb window. C) The mean wRF of all ~~10kb~~10 kb window trees within each 5Mb window compared to the species tree.

Figure 5

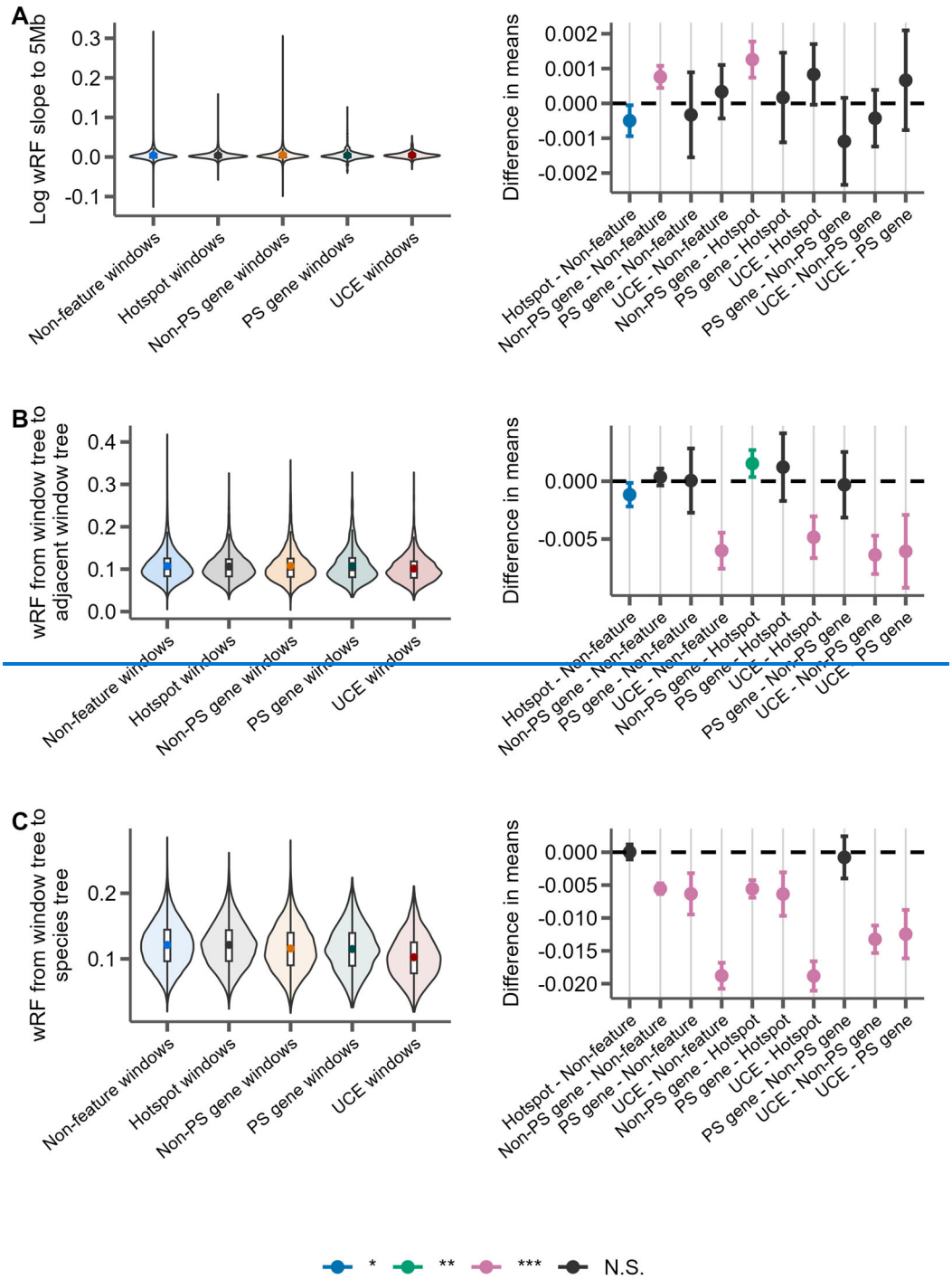
A
Log wRF slope to 5Mb
0.3
0.2
0.1
0.0
-0.1
Non-feature windows
Hotspot windows
Non-PS gene windows
PS gene windows
UCE windows
Difference in means
0.002
0.001
0.000
-0.001
-0.002
Hotspot - Non-feature
Non-PS gene - Non-feature
PS gene - Non-feature
UCE - Non-feature
Non-PS gene - Hotspot
PS gene - Hotspot
UCE - Hotspot
PS gene - Non-PS gene
UCE - Non-PS gene
UCE - PS gene
B
wRF from window tree to adjacent window tree
0.4
0.3
0.2
0.1
0.0
Non-feature windows
Hotspot windows
Non-PS gene windows
PS gene windows
UCE windows
Difference in means
0.000
-0.005
Hotspot - Non-feature
Non-PS gene - Non-feature
PS gene - Non-feature
UCE - Non-feature
Non-PS gene - Hotspot
PS gene - Hotspot
UCE - Hotspot
PS gene - Non-PS gene
UCE - Non-PS gene
UCE - PS gene
C
wRF from window tree to species tree
0.2
0.1
Non-feature windows
Hotspot windows
Non-PS gene windows
PS gene windows
UCE windows
Difference in means
0.000
-0.005
-0.010
-0.015
-0.020
Hotspot - Non-feature
Non-PS gene - Non-feature
PS gene - Non-feature
UCE - Non-feature
Non-PS gene - Hotspot
PS gene - Hotspot
UCE - Hotspot
PS gene - Non-PS gene
UCE - Non-PS gene
UCE - PS gene
*
**
***
N.S.

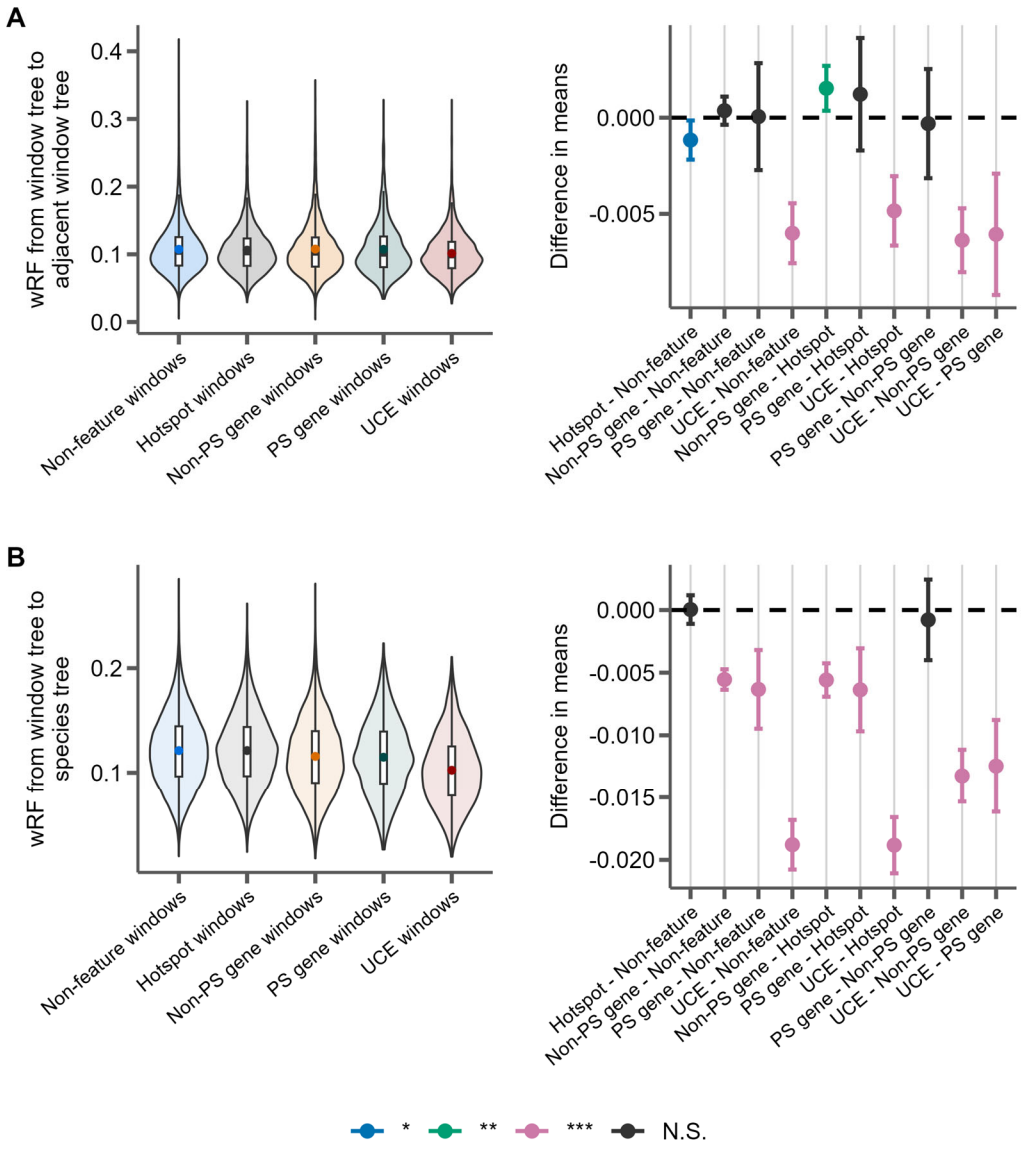

Figure 5: Distributions of weighted Robinson-Foulds distance from trees constructed from 10kb windows either centered on recombination hotspots (Hotspot), protein-coding genes without evidence for positive selection (Non-PS genes), protein coding genes with evidence for positive selection (PS genes), UCEs, or containing none of these features (Non-feature). For each panel, the left portion shows the distributions of the measure for each feature type and the right panel shows the differences in means for each pairwise comparison of features with significance assessed with Tukey's range test. The labels on the x-axis indicate the feature pairs being compared, with the first feature being the reference (*i.e.* points above 0 indicate this feature has a higher mean). *P*-value thresholds: * < 0.05, ** < 0.01, *** <0.001. ~~A) The rate of decay of phylogenetic similarity is calculated as the slope of a linear regression between wRF and the log distance between each window up to 5Mb away from the feature window. B~~A) The phylogenetic similarity of windows

immediately adjacent to feature windows. ~~C~~B) The phylogenetic similarity between the species tree inferred from protein-coding gene trees and the feature window.

Figure 6

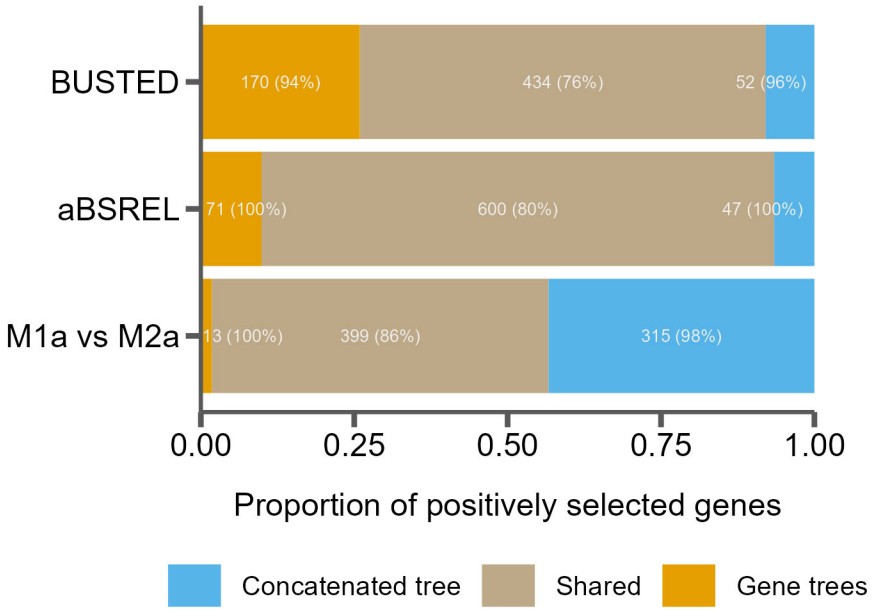

Figure 6. Tree misspecification leads to erroneous results in tests for positive selection. The proportion of genes inferred to be under positive selection for three tests using either a single species tree (concatenated tree) or individual gene trees, as well as those found in both cases (shared). Numbers in the bars indicate raw counts, and percentages indicate the percent of genes in that category that are discordant from the species tree.

References

PDB (The Paleobiology Database) [Internet]. 2011 January 21st, 2022]. Available from: http://paleodb.org/

Aghova T, Kimura Y, Bryja J, Dobigny G, Granjon L, Kergoat GJ. 2018. Fossils know it best: Using a new set of fossil calibrations to improve the temporal phylogenetic framework of murid rodents (Rodentia: Muridae). Mol Phylogenet Evol 128:98-111.

Alda F, Ludt WB, Elias DJ, McMahan CD, Chakrabarty P. 2021. Comparing Ultraconserved Elements and Exons for Phylogenomic Analyses of Middle American Cichlids: When Data Agree to Disagree. Genome Biol Evol 13:evab161.

Alexander AM, Su YC, Oliveros CH, Olson KV, Travers SL, Brown RM. 2017. Genomic data reveals potential for hybridization, introgression, and incomplete lineage sorting to confound phylogenetic relationships in an adaptive radiation of narrow-mouth frogs. Evolution 71:475-488.

Avise JC, Robinson TJ. 2008. Hemiplasy: a new term in the lexicon of phylogenetics. Syst Biol 57:503-507.

Baudat F, Buard J, Grey C, Fledel-Alon A, Ober C, Przeworski M, Coop G, de Massy B. 2010. PRDM9 is a major determinant of meiotic recombination hotspots in humans and mice. Science 327:836-840.

Baum DA. 2007. Concordance trees, concordance factors, and the exploration of reticulate genealogy. TAXON 56:417-426.

Benjamini Y, Hochberg Y. 1995. Controlling the false discovery rate: a practical and powerful approach to multiple testing. Journal of the Royal statistical society: series B (Methodological) 57:289-300.

Bloom BH. 1970. Space/time trade-offs in hash coding with allowable errors. Commun. ACM 13:422–426.

Böcker S, Canzar S, Gunnar WK. 2013. The Generalized Robinson-Foulds Metric. In: Darling A, Stoye J, editors. Algorithms in Bioinformatics. Berlin, Heidelberg: Springer.

Bolger AM, Lohse M, Usadel B. 2014. Trimmomatic: a flexible trimmer for Illumina sequence data. Bioinformatics 30:2114-2120.

Borowiec ML. 2016. AMAS: a fast tool for alignment manipulation and computing of summary statistics. PeerJ 4:e1660.

Bradley RK, Roberts A, Smoot M, Juvekar S, Do J, Dewey C, Holmes I, Pachter L. 2009. Fast statistical alignment. PLoS Comput Biol 5:e1000392.

Capella-Gutierrez S, Silla-Martinez JM, Gabaldon T. 2009. trimAl: a tool for automated alignment trimming in large-scale phylogenetic analyses. Bioinformatics 25:1972-1973.

Carbone L, Harris RA, Gnerre S, Veeramah KR, Lorente-Galdos B, Huddleston J, Meyer TJ, Herrero J, Roos C, Aken B, et al. 2014. Gibbon genome and the fast karyotype evolution of small apes. Nature 513:195-201.

Chan KO, Hutter CR, Wood PL, Jr., Grismer LL, Brown RM. 2020. Target-capture phylogenomics provide insights on gene and species tree discordances in Old World treefrogs (Anura: Rhacophoridae). Proc Biol Sci 287:20202102.

Charlesworth B, Morgan MT, Charlesworth D. 1993. The effect of deleterious mutations on neutral molecular variation. Genetics 134:1289-1303.

Chernomor O, von Haeseler A, Minh BQ. 2016. Terrace Aware Data Structure for Phylogenomic Inference from Supermatrices. Syst Biol 65:997-1008.

Christmas MJ, Kaplow IM, Genereux DP, Dong MX, Hughes GM, Li X, Sullivan PF, Hindle AG, Andrews G, Armstrong JC, et al. 2023. Evolutionary constraint and innovation across hundreds of placental mammals. Science 380:eabn3943.

Cox A, Ackert-Bicknell CL, Dumont BL, Ding Y, Bell JT, Brockmann GA, Wergedal JE, Bult C, Paigen B, Flint J, et al. 2009. A new standard genetic map for the laboratory mouse. Genetics 182:1335-1344.

Cunningham F, Allen JE, Allen J, Alvarez-Jarreta J, Amode MR, Armean IM, Austine-Orimoloye O, Azov AG, Barnes I, Bennett R, et al. 2022. Ensembl 2022. Nucleic Acids Res 50:D988-D995.

Danecek P, Bonfield JK, Liddle J, Marshall J, Ohan V, Pollard MO, Whitwham A, Keane T, McCarthy SA, Davies RM, et al. 2021. Twelve years of SAMtools and BCFtools. Gigascience 10:giab008.

Dapper AL, Payseur BA. 2017. Connecting theory and data to understand recombination rate evolution. Philos Trans R Soc Lond B Biol Sci 372.

Daxner-Höck G. 2002. Cricetodon meini and other rodents from Mühlbach and Grund, Lower Austria (Middle Miocene, late MN5). Annalen des Naturhistorischen Museums in Wien. Serie A für Mineralogie und Petrographie, Geologie und Paläontologie, Anthropologie und Prähistorie:267-291.

Degnan JH, Rosenberg NA. 2006. Discordance of species trees with their most likely gene trees. PLoS Genet 2:e68.

Edwards SV. 2009. Is a new and general theory of molecular systematics emerging? Evolution 63:1-19.

Faircloth BC. 2013. illumiprocessor: a trimmomatic wrapper for parallel adapter and quality trimming.

Faircloth BC. 2016. PHYLUCE is a software package for the analysis of conserved genomic loci. Bioinformatics 32:786-788.

Faircloth BC, McCormack JE, Crawford NG, Harvey MG, Brumfield RT, Glenn TC. 2012. Ultraconserved elements anchor thousands of genetic markers spanning multiple evolutionary timescales. Syst Biol 61:717-726.

Feng S, Bai M, Rivas-Gonzalez I, Li C, Liu S, Tong Y, Yang H, Chen G, Xie D, Sears KE, et al. 2022. Incomplete lineage sorting and phenotypic evolution in marsupials. Cell 185:1646-1660 e1618.

Ferreira MS, Jones MR, Callahan CM, Farelo L, Tolesa Z, Suchentrunk F, Boursot P, Mills LS, Alves PC, Good JM, et al. 2021. The Legacy of Recurrent Introgression during the Radiation of Hares. Syst Biol 70:593-607.

Foley NM, Harris AJ, Bredemeyer KR, Ruedi M, Puechmaille SJ, Teeling EC, Criscitiello MF, Murphy WJ. 2024. Karyotypic stasis and swarming influenced the evolution of viral tolerance in a species-rich bat radiation. Cell Genom 4:100482.

Foley NM, Mason VC, Harris AJ, Bredemeyer KR, Damas J, Lewin HA, Eizirik E, Gatesy J, Karlsson EK, Lindblad-Toh K, et al. 2023. A genomic timescale for placental mammal evolution. Science 380:eabl8189.

Fontaine MC, Pease JB, Steele A, Waterhouse RM, Neafsey DE, Sharakhov IV, Jiang X, Hall AB, Catteruccia F, Kakani E, et al. 2015. Mosquito genomics. Extensive introgression in a malaria vector species complex revealed by phylogenomics. Science 347:1258524.

Foote AD, Liu Y, Thomas GW, Vinar T, Alfoldi J, Deng J, Dugan S, van Elk CE, Hunter ME, Joshi V, et al. 2015. Convergent evolution of the genomes of marine mammals. Nat Genet 47:272-275.

Gable SM, Byars MI, Literman R, Tollis M. 2022. A Genomic Perspective on the Evolutionary Diversification of Turtles. Syst Biol 71:1331-1347.

Gibbs RA, Weinstock GM, Metzker ML, Muzny DM, Sodergren EJ, Scherer S, Scott G, Steffen D, Worley KC, Burch PE, et al. 2004. Genome sequence of the Brown Norway rat yields insights into mammalian evolution. Nature 428:493-521.

Good JM, Wiebe V, Albert FW, Burbano HA, Kircher M, Green RE, Halbwax M, Andre C, Atencia R, Fischer A, et al. 2013. Comparative population genomics of the ejaculate in humans and the great apes. Mol Biol Evol 30:964-976.

Green RE, Krause J, Briggs AW, Maricic T, Stenzel U, Kircher M, Patterson N, Li H, Zhai W, Fritz MH, et al. 2010. A draft sequence of the Neandertal genome. Science 328:710-722.

Guindon S, Dufayard JF, Lefort V, Anisimova M, Hordijk W, Gascuel O. 2010. New algorithms and methods to estimate maximum-likelihood phylogenies: assessing the performance of PhyML 3.0. Syst Biol 59:307-321.

Hahn MW, Nakhleh L. 2016. Irrational exuberance for resolved species trees. Evolution 70:7-17.

He B, Zhao Y, Su C, Lin G, Wang Y, Li L, Ma J, Yang Q, Hao J. 2023. Phylogenomics reveal extensive phylogenetic discordance due to incomplete lineage sorting following the rapid radiation of alpine butterflies (Papilionidae: Parnassius). Syst Entomol.

Hibbins MS, Breithaupt LC, Hahn MW. 2023. Phylogenomic comparative methods: Accurate evolutionary inferences in the presence of gene tree discordance. Proc Natl Acad Sci U S A 120:e2220389120.

Hinrichs AS, Karolchik D, Baertsch R, Barber GP, Bejerano G, Clawson H, Diekhans M, Furey TS, Harte RA, Hsu F, et al. 2006. The UCSC Genome Browser Database: update 2006. Nucleic Acids Res 34:D590-598.

Hoang DT, Chernomor O, von Haeseler A, Minh BQ, Vinh LS. 2018. UFBoot2: Improving the Ultrafast Bootstrap Approximation. Mol Biol Evol 35:518-522.

Hobolth A, Christensen OF, Mailund T, Schierup MH. 2007. Genomic relationships and speciation times of human, chimpanzee, and gorilla inferred from a coalescent hidden Markov model. PLoS Genet 3:e7.

Holm S. 1979. A simple sequentially rejective multiple test procedure. Scandinavian journal of statistics:65-70.

Hu Z, Sackton TB, Edwards SV, Liu JS. 2019. Bayesian Detection of Convergent Rate Changes of Conserved Noncoding Elements on Phylogenetic Trees. Mol Biol Evol 36:1086-1100.

Hudson RR. 1983. Testing the Constant-Rate Neutral Allele Model with Protein Sequence Data. Evolution 37:203-217.

Hudson RR, Kaplan NL. 1988. The coalescent process in models with selection and recombination. Genetics 120:831-840.

Hudson RR, Kaplan NL. 1995. Deleterious background selection with recombination. Genetics 141:1605-1617.

Huson DH, Klöpper T, Lockhart PJ, Steel MA. 2005. Reconstruction of Reticulate Networks from Gene Trees. In: Miyano S, Mesirov J, Kasif S, Istrail S, Pevzner PA, Waterman M, editors. Research in Computational Molecular Biology. RECOMB 2005. Lecture Notes in Computer Science: Springer, Berlin, Heidelberg.

Jackman SD, Vandervalk BP, Mohamadi H, Chu J, Yeo S, Hammond SA, Jahesh G, Khan H, Coombe L, Warren RL, et al. 2017. ABySS 2.0: resource-efficient assembly of large genomes using a Bloom filter. Genome Res 27:768-777.

Jarvis ED, Mirarab S, Aberer AJ, Li B, Houde P, Li C, Ho SY, Faircloth BC, Nabholz B, Howard JT, et al. 2014. Whole-genome analyses resolve early branches in the tree of life of modern birds. Science 346:1320-1331.

Jensen-Seaman MI, Furey TS, Payseur BA, Lu Y, Roskin KM, Chen CF, Thomas MA, Haussler D, Jacob HJ. 2004. Comparative recombination rates in the rat, mouse, and human genomes. Genome Res 14:528-538.

Jones MR, Mills LS, Alves PC, Callahan CM, Alves JM, Lafferty DJR, Jiggins FM, Jensen JD, Melo-Ferreira J, Good JM. 2018. Adaptive introgression underlies polymorphic seasonal camouflage in snowshoe hares. Science 360:1355-1358.

Junier T, Zdobnov EM. 2010. The Newick utilities: high-throughput phylogenetic tree processing in the UNIX shell. Bioinformatics 26:1669-1670.

Kalyaanamoorthy S, Minh BQ, Wong TKF, von Haeseler A, Jermiin LS. 2017. ModelFinder: fast model selection for accurate phylogenetic estimates. Nat Methods 14:587-589.

Kaplan NL, Hudson RR, Langley CH. 1989. The "hitchhiking effect" revisited. Genetics 123:887-899.

Kartje ME, Jing P, Payseur BA. 2020. Weak Correlation between Nucleotide Variation and Recombination Rate across the House Mouse Genome. Genome Biol Evol 12:293-299.

Katoh K, Standley DM. 2013. MAFFT multiple sequence alignment software version 7: improvements in performance and usability. Mol Biol Evol 30:772-780.

Katzman S, Kern AD, Bejerano G, Fewell G, Fulton L, Wilson RK, Salama SR, Haussler D. 2007. Human genome ultraconserved elements are ultraselected. Science 317:915.

Keane TM, Wong K, Adams DJ, Flint J, Reymond A, Yalcin B. 2014. Identification of structural variation in mouse genomes. Front Genet 5:192.

Kimura Y, Hawkins MT, McDonough MM, Jacobs LL, Flynn LJ. 2015. Corrected placement of Mus-Rattus fossil calibration forces precision in the molecular tree of rodents. Sci Rep 5:14444.

Kimura Y, Jacobs LL, Cerling TE, Uno KT, Ferguson KM, Flynn LJ, Patnaik R. 2013. Fossil mice and rats show isotopic evidence of niche partitioning and change in dental ecomorphology related to dietary shift in Late Miocene of Pakistan. PLoS One 8:e69308.

1051 Kong A, Gudbjartsson DF, Sainz J, Jonsdottir GM, Gudjonsson SA, Richardsson B, Sigurdardottir
1052 S, Barnard J, Hallbeck B, Masson G, et al. 2002. A high-resolution recombination map of the
1053 human genome. Nat Genet 31:241-247.

1054
1055 Kowalczyk A, Meyer WK, Partha R, Mao W, Clark NL, Chikina M. 2019. RERconverge: an R
1056 package for associating evolutionary rates with convergent traits. Bioinformatics 35:4815-4817.

1057
1058 Kulathinal RJ, Stevison LS, Noor MA. 2009. The genomics of speciation in Drosophila: diversity,
1059 divergence, and introgression estimated using low-coverage genome sequencing. PLoS Genet
1060 5:e1000550.

1061
1062 Kumon T, Ma J, Akins RB, Stefanik D, Nordgren CE, Kim J, Levine MT, Lampson MA. 2021.
1063 Parallel pathways for recruiting effector proteins determine centromere drive and suppression. Cell
1064 184:4904-4918 e4911.

1065
1066 Calculating and interpreting gene- and site-concordance factors in phylogenomics [Internet]. The
1067 Lanfear Lab @ ANU2018 September 20, 2021]. Available from:
1068 http://www.robertlanfear.com/blog/files/concordance_factors.html

1069
1070 Lecompte E, Aplin K, Denys C, Catzeflis F, Chades M, Chevret P. 2008. Phylogeny and
1071 biogeography of African Murinae based on mitochondrial and nuclear gene sequences, with a new
1072 tribal classification of the subfamily. BMC Evol Biol 8:199.

1073
1074 Lewontin RC, Birch LC. 1966. Hybridization as a Source of Variation for Adaptation to New
1075 Environments. Evolution 20:315-336.

1076
1077 Li H. 2013. Aligning sequence reads, clone sequences and assembly contigs with BWA-MEM.
1078 arXiv preprint arXiv:1303.3997.

1079
1080 Li H. 2018. Minimap2: pairwise alignment for nucleotide sequences. Bioinformatics 34:3094-
1081 3100.

1082
1083 Liu X, Wei F, Li M, Jiang X, Feng Z, Hu J. 2004. Molecular phylogeny and taxonomy of wood
1084 mice (genus Apodemus Kaup, 1829) based on complete mtDNA cytochrome b sequences, with
1085 emphasis on Chinese species. Mol Phylogenet Evol 33:1-15.

1086
1087 Lopes F, Oliveira LR, Kessler A, Beux Y, Crespo E, Cardenas-Alayza S, Majluf P, Sepulveda M,
1088 Brownell RL, Franco-Trecu V, et al. 2021. Phylogenomic Discordance in the Eared Seals is best

explained by Incomplete Lineage Sorting following Explosive Radiation in the Southern Hemisphere. Syst Biol 70:786-802.

Lundrigan BL, Jansa SA, Tucker PK. 2002. Phylogenetic relationships in the genus mus, based on paternally, maternally, and biparentally inherited characters. Syst Biol 51:410-431.

Maddison WP. 1997. Gene Trees in Species Trees. Systematic Biology 46:523-536.

Martin Y, Gerlach G, Schlotterer C, Meyer A. 2000. Molecular phylogeny of European muroid rodents based on complete cytochrome b sequences. Mol Phylogenet Evol 16:37-47.

McKenzie PF, Eaton DAR. 2020. The Multispecies Coalescent in Space and Time. bioRxiv:2020.2008.2002.233395.

Mendes FK, Fuentes-Gonzalez JA, Schraiber JG, Hahn MW. 2018. A multispecies coalescent model for quantitative traits. Elife 7:e36482.

Mendes FK, Hahn MW. 2016. Gene Tree Discordance Causes Apparent Substitution Rate Variation. Syst Biol 65:711-721.

Mendes FK, Hahn Y, Hahn MW. 2016. Gene Tree Discordance Can Generate Patterns of Diminishing Convergence over Time. Mol Biol Evol 33:3299-3307.

Mendes FK, Livera AP, Hahn MW. 2019. The perils of intralocus recombination for inferences of molecular convergence. Philos Trans R Soc Lond B Biol Sci 374:20180244.

Mikula O, Nicolas V, Šumbera R, Konečný A, Denys C, Verheyen E, Bryjová A, Lemmon AR, Lemmon EM, Bryja J. 2021. Nuclear phylogenomics, but not mitogenomics, resolves the most successful Late Miocene radiation of African mammals (Rodentia: Muridae: Arvicanthini). Molecular Phylogenetics and Evolution 157:107069.

Minh BQ, Hahn MW, Lanfear R. 2020. New Methods to Calculate Concordance Factors for Phylogenomic Datasets. Mol Biol Evol 37:2727-2733.

Minh BQ, Schmidt HA, Chernomor O, Schrempf D, Woodhams MD, von Haeseler A, Lanfear R. 2020. IQ-TREE 2: New Models and Efficient Methods for Phylogenetic Inference in the Genomic Era. Mol Biol Evol 37:1530-1534.

Mölder F, Jablonski KP, Letcher B, Hall MB, Tomkins-Tinch CH, Sochat V, Forster J, Lee S, Twardziok SO, Kanitz A, et al. 2021. Sustainable data analysis with Snakemake. F1000Res 10:33.

Moore EC, Thomas GWC, Mortimer S, Kopania EEK, Hunnicutt KE, Clare-Salzler ZJ, Larson EL, Good JM. 2022. The Evolution of Widespread Recombination Suppression on the Dwarf Hamster (Phodopus) X Chromosome. Genome Biol Evol 14:evac080.

Mouse Genome Sequencing C, Waterston RH, Lindblad-Toh K, Birney E, Rogers J, Abril JF, Agarwal P, Agarwala R, Ainscough R, Alexandersson M, et al. 2002. Initial sequencing and comparative analysis of the mouse genome. Nature 420:520-562.

Murrell B, Weaver S, Smith MD, Wertheim JO, Murrell S, Aylward A, Eren K, Pollner T, Martin DP, Smith DM, et al. 2015. Gene-wide identification of episodic selection. Mol Biol Evol 32:1365-1371.

Nilsson P, Solbakken MH, Schmid BV, Orr RJS, Lv R, Cui Y, Song Y, Zhang Y, Baalsrud HT, Torresen OK, et al. 2020. The Genome of the Great Gerbil Reveals Species-Specific Duplication of an MHCII Gene. Genome Biol Evol 12:3832-3849.

Pagès M, Fabre P-H, Chaval Y, Mortelliti A, Nicolas V, Wells K, Michaux JR, Lazzari V. 2016. Molecular phylogeny of South-East Asian arboreal murine rodents. Zoologica Scripta 45:349-364.

Pamilo P, Nei M. 1988. Relationships between gene trees and species trees. Mol Biol Evol 5:568-583.

Paradis E, Schliep K. 2019. ape 5.0: an environment for modern phylogenetics and evolutionary analyses in R. Bioinformatics 35:526-528.

Partha R, Kowalczyk A, Clark NL, Chikina M. 2019. Robust Method for Detecting Convergent Shifts in Evolutionary Rates. Mol Biol Evol 36:1817-1830.

Pease JB, Haak DC, Hahn MW, Moyle LC. 2016. Phylogenomics Reveals Three Sources of Adaptive Variation during a Rapid Radiation. PLoS Biol 14:e1002379.

Pease JB, Hahn MW. 2013. More accurate phylogenies inferred from low-recombination regions in the presence of incomplete lineage sorting. Evolution 67:2376-2384.

Platt RN, 2nd, Vandewege MW, Ray DA. 2018. Mammalian transposable elements and their impacts on genome evolution. Chromosome Res 26:25-43.

Pollard KS, Hubisz MJ, Rosenbloom KR, Siepel A. 2010. Detection of nonneutral substitution rates on mammalian phylogenies. Genome Res 20:110-121.

Pond SL, Frost SD, Muse SV. 2005. HyPhy: hypothesis testing using phylogenies. Bioinformatics 21:676-679.

Poplin R, Ruano-Rubio V, DePristo MA, Fennell TJ, Carneiro MO, Auwera GAVd, Kling DE, Gauthier LD, Levy-Moonshine A, Roazen D, et al. 2018. Scaling accurate genetic variant discovery to tens of thousands of samples. bioRxiv:201178.

Ptak SE, Hinds DA, Koehler K, Nickel B, Patil N, Ballinger DG, Przeworski M, Frazer KA, Paabo S. 2005. Fine-scale recombination patterns differ between chimpanzees and humans. Nat Genet 37:429-434.

Quinlan AR, Hall IM. 2010. BEDTools: a flexible suite of utilities for comparing genomic features. Bioinformatics 26:841-842.

R Core Team. 2021. R: A language and environment for statistical computing. Vienna, Austria.

Ranwez V, Douzery EJP, Cambon C, Chantret N, Delsuc F. 2018. MACSE v2: Toolkit for the Alignment of Coding Sequences Accounting for Frameshifts and Stop Codons. Mol Biol Evol 35:2582-2584.

Revell LJ. 2012. phytools: an R package for phylogenetic comparative biology (and other things). Methods in Ecology and Evolution 3:217-223.

Rivas-Gonzalez I, Rousselle M, Li F, Zhou L, Dutheil JY, Munch K, Shao Y, Wu D, Schierup MH, Zhang G. 2023. Pervasive incomplete lineage sorting illuminates speciation and selection in primates. Science 380:eabn4409.

Robinson DF, Foulds LR. 1981. Comparison of phylogenetic trees. Mathematical Biosciences 53:131-147.

Robinson DF, Foulds LR editors.; 1979 Berlin, Heidelberg.

Romanenko SA, Perelman PL, Trifonov VA, Graphodatsky AS. 2012. Chromosomal evolution in Rodentia. Heredity (Edinb) 108:4-16.

Rosenberg NA. 2002. The probability of topological concordance of gene trees and species trees. Theor Popul Biol 61:225-247.

Rowe KC, Achmadi AS, Fabre P-H, Schenk JJ, Steppan SJ, Esselstyn JA. 2019. Oceanic islands of Wallacea as a source for dispersal and diversification of murine rodents. Journal of Biogeography 46:2752-2768.

Roycroft E, Achmadi A, Callahan CM, Esselstyn JA, Good JM, Moussalli A, Rowe KC. 2021. Molecular Evolution of Ecological Specialisation: Genomic Insights from the Diversification of Murine Rodents. Genome Biol Evol 13:evab103.

Roycroft EJ, Moussalli A, Rowe KC. 2020. Phylogenomics Uncovers Confidence and Conflict in the Rapid Radiation of Australo-Papuan Rodents. Syst Biol 69:431-444.

Sarver BA, Keeble S, Cosart T, Tucker PK, Dean MD, Good JM. 2017. Phylogenomic Insights into Mouse Evolution Using a Pseudoreference Approach. Genome Biol Evol 9:726-739.

Scally A, Dutheil JY, Hillier LW, Jordan GE, Goodhead I, Herrero J, Hobolth A, Lappalainen T, Mailund T, Marques-Bonet T, et al. 2012. Insights into hominid evolution from the gorilla genome sequence. Nature 483:169-175.

Schenk JJ, Rowe KC, Steppan SJ. 2013. Ecological opportunity and incumbency in the diversification of repeated continental colonizations by muroid rodents. Syst Biol 62:837-864.

Schliep KP. 2011. phangorn: phylogenetic analysis in R. Bioinformatics 27:592-593.

Serizawa K, Suzuki H, Tsuchiya K. 2000. A phylogenetic view on species radiation in Apodemus inferred from variation of nuclear and mitochondrial genes. Biochem Genet 38:27-40.

Shifman S, Bell JT, Copley RR, Taylor MS, Williams RW, Mott R, Flint J. 2006. A high-resolution single nucleotide polymorphism genetic map of the mouse genome. PLoS Biol 4:e395.

Singhal S, Leffler EM, Sannareddy K, Turner I, Venn O, Hooper DM, Strand AI, Li Q, Raney B, Balakrishnan CN, et al. 2015. Stable recombination hotspots in birds. Science 350:928-932.

1240 Slatkin M, Pollack JL. 2006. The concordance of gene trees and species trees at two linked loci.
1241 Genetics 172:1979-1984.

1242
1243 Smagulova F, Gregoretti IV, Brick K, Khil P, Camerini-Otero RD, Petukhova GV. 2011. Genome-
1244 wide analysis reveals novel molecular features of mouse recombination hotspots. Nature 472:375-
1245 378.

1246
1247 RepeatMasker Open-4.0 [Internet]. 2013-2015. Available from http://www.repeatmasker.org.

1248
1249 Smith BT, Merwin J, Provost KL, Thom G, Brumfield RT, Ferreira M, Mauck WM, Moyle RG,
1250 Wright TF, Joseph L. 2023. Phylogenomic Analysis of the Parrots of the World Distinguishes
1251 Artifactual from Biological Sources of Gene Tree Discordance. Syst Biol 72:228-241.

1252
1253 Smith JM, Haigh J. 1974. The hitch-hiking effect of a favourable gene. Genet Res 23:23-35.

1254
1255 Smith MD, Wertheim JO, Weaver S, Murrell B, Scheffler K, Kosakovsky Pond SL. 2015. Less is
1256 more: an adaptive branch-site random effects model for efficient detection of episodic diversifying
1257 selection. Mol Biol Evol 32:1342-1353.

1258
1259 Smith SA, Brown JW, Walker JF. 2018. So many genes, so little time: A practical approach to
1260 divergence-time estimation in the genomic era. PLoS One 13:e0197433.

1261
1262 Smith SA, Moore MJ, Brown JW, Yang Y. 2015. Analysis of phylogenomic datasets reveals
1263 conflict, concordance, and gene duplications with examples from animals and plants. BMC Evol
1264 Biol 15:150.

1265
1266 Stanyon R, Yang F, Cavagna P, O'Brien P, Bagga M, Ferguson-Smith M, Wienberg J. 1999.
1267 Animal Cytogenetics and Comparative Mapping-Reciprocal chromosome painting shows that
1268 genomic rearrangement between rat and mouse proceeds ten times faster than between humans
1269 and cats. Cytogenetics and Cell Genetics 84:150-155.

1270
1271 Stapley J, Feulner PGD, Johnston SE, Santure AW, Smadja CM. 2017. Variation in recombination
1272 frequency and distribution across eukaryotes: patterns and processes. Philos Trans R Soc Lond B
1273 Biol Sci 372.

1274
1275 Steppan SJ, Adkins RM, Spinks PQ, Hale C. 2005. Multigene phylogeny of the Old World mice,
1276 Murinae, reveals distinct geographic lineages and the declining utility of mitochondrial genes
1277 compared to nuclear genes. Mol Phylogenet Evol 37:370-388.

Steppan SJ, Schenk JJ. 2017. Muroid rodent phylogenetics: 900-species tree reveals increasing diversification rates. PLoS One 12:e0183070.

Stevison LS, Woerner AE, Kidd JM, Kelley JL, Veeramah KR, McManus KF, Great Ape Genome P, Bustamante CD, Hammer MF, Wall JD. 2016. The Time Scale of Recombination Rate Evolution in Great Apes. Mol Biol Evol 33:928-945.

Sun C, Huang J, Wang Y, Zhao X, Su L, Thomas GWC, Zhao M, Zhang X, Jungreis I, Kellis M, et al. 2021. Genus-Wide Characterization of Bumblebee Genomes Provides Insights into Their Evolution and Variation in Ecological and Behavioral Traits. Mol Biol Evol 38:486-501.

Suzuki H, Shimada T, Terashima M, Tsuchiya K, Aplin K. 2004. Temporal, spatial, and ecological modes of evolution of Eurasian Mus based on mitochondrial and nuclear gene sequences. Mol Phylogenet Evol 33:626-646.

Tange O. 2018. GNU Parallel.

To TH, Jung M, Lycett S, Gascuel O. 2016. Fast Dating Using Least-Squares Criteria and Algorithms. Syst Biol 65:82-97.

Treaster S, Deelen J, Daane JM, Murabito J, Karasik D, Harris MP. 2023. Convergent genomics of longevity in rockfishes highlights the genetics of human life span variation. Sci Adv 9:eadd2743.

van der Valk T, Pecnerova P, Diez-Del-Molino D, Bergstrom A, Oppenheimer J, Hartmann S, Xenikoudakis G, Thomas JA, Dehasque M, Saglican E, et al. 2021. Million-year-old DNA sheds light on the genomic history of mammoths. Nature 591:265-269.

Vanderpool D, Minh BQ, Lanfear R, Hughes D, Murali S, Harris RA, Raveendran M, Muzny DM, Hibbins MS, Williamson RJ, et al. 2020. Primate phylogenomics uncovers multiple rapid radiations and ancient interspecific introgression. PLoS Biol 18:e3000954.

Wang LG, Lam TT, Xu S, Dai Z, Zhou L, Feng T, Guo P, Dunn CW, Jones BR, Bradley T, et al. 2020. Treeio: An R Package for Phylogenetic Tree Input and Output with Richly Annotated and Associated Data. Mol Biol Evol 37:599-603.

White MA, Ane C, Dewey CN, Larget BR, Payseur BA. 2009. Fine-scale phylogenetic discordance across the house mouse genome. PLoS Genet 5:e1000729.

Yalcin B, Wong K, Agam A, Goodson M, Keane TM, Gan X, Nellaker C, Goodstadt L, Nicod J, Bhomra A, et al. 2011. Sequence-based characterization of structural variation in the mouse genome. Nature 477:326-329.

Yang Z. 2007. PAML 4: phylogenetic analysis by maximum likelihood. Mol Biol Evol 24:1586-1591.

Yekutieli D, Benjamini Y. 1999. Resampling-based false discovery rate controlling multiple test procedures for correlated test statistics. Journal of Statistical Planning and Inference 82:171-196.

Yu G. 2020. Using ggtree to Visualize Data on Tree-Like Structures. Curr Protoc Bioinformatics 69:e96.

Yu G, Smith DK, Zhu H, Guan Y, Lam TT-Y. 2017. ggtree: an r package for visualization and annotation of phylogenetic trees with their covariates and other associated data. Methods in Ecology and Evolution 8:28-36.

Zhang C, Rabiee M, Sayyari E, Mirarab S. 2018. ASTRAL-III: polynomial time species tree reconstruction from partially resolved gene trees. BMC Bioinformatics 19:153.